Zuerst ersch. in : British Journal of Pharmacology ; 152 (2007), 6. - S. 959–979
DOI : 10.1038/sj.bjp.0707471

RESEARCH PAPER

Efficacy of small-molecule glycogen synthase kinase-3 inhibitors in the postnatal rat model of tau hyperphosphorylation

M-L Selenica[1], HS Jensen[1], AK Larsen[2], ML Pedersen[3], L Helboe[1], M Leist[4] and J Lotharius[1]

[1]*Division of Biological Research, H Lundbeck A/S, Copenhagen, Denmark;* [2]*Division of Clinical Research, Neurology, H Lundbeck A/S, Copenhagen, Denmark;* [3]*Department of Metabolism, H Lundbeck A/S, Copenhagen, Denmark and* [4]*Faculty of Biology, University of Konstanz, Konstanz, Germany*

Background and purpose: Glycogen synthase kinase-3 (GSK-3) affects neuropathological events associated with Alzheimeŕs disease (AD) such as hyperphosphorylation of the protein, tau. GSK-3β expression, enzyme activity and tau phosphorylated at AD-relevant epitopes are elevated in juvenile rodent brains. Here, we assess five GSK-3β inhibitors and lithium in lowering phosphorylated tau (p-tau) and GSK-3β enzyme activity levels in 12-day old postnatal rats.
Experimental approach: Brain levels of inhibitors following treatment *in vivo* were optimized based on pharmacokinetic data. At optimal doses, p-tau (Ser^{396}) levels in brain tissue was measured by immunoblotting and correlated with GSK-3β enzyme activities in the same tissues. Effects of GSK inhibitors on p-tau, GSK-3β activities and cell death were measured in a human neuronal cell line (LUHMES).
Key results: Lithium and CHIR98014 reduced tau phosphorylation (Ser^{396}) in the cortex and hippocampus of postnatal rats, while Alsterpaullone and SB216763 were effective only in hippocampus. AR-A014418 and Indirubin-3′-monoxime were ineffective in either brain region. Inhibition of p-tau in brain required several-fold higher levels of GSK inhibitors than the IC_{50} values obtained in recombinant or cell-based GSK-3β enzyme activity assays. The inhibitory effect on GSK-3β activity *ex vivo* correlated with protection against cell death and decrease of p-tau- in LUHMES cells, using low μM inhibitor concentrations.
Conclusions and Implications: Selective small-molecule inhibitors of GSK-3 reduce tau phosphorylation *in vivo*. These findings corroborate earlier suggestions that GSK-3β may be an attractive target for disease-modification in AD and related conditions where tau phosphorylation is believed to contribute to disease pathogenesis.

Keywords: phosphorylated tau; AR-A014418; SB216763; CHIR98014; Indirubin-3′-monoxime; Alsterpaullone; LiCl

Abbreviations: Aβ, amyloid-β; CDK2/5, cyclin-dependent kinase 2/5; FTDP-17, fronto-temporal dementia linked to chromosome 17; GSK-3β, glycogen synthase kinase-3β; HTLC, high turbulent liquid flow chromatography; MS/MS, mass spectrometry; NFT, neurofibrillary tangles; p-tau, phosphorylated tau; P-12, postnatal day 12; PI3 kinase, phosphatidyl-inositol 3 kinase; PP-2A/B, protein phosphatases 2A/B

Introduction

Alzheimer's disease (AD) is a neurodegenerative condition characterized by the extracellular accumulation of senile plaques and intraneuronal formation of neurofibrillary tangles (NFT) (Braak and Braak, 1991; Iqbal *et al*., 2005). The protein tau promotes microtubule assembly (Weingarten *et al*., 1975) and stabilization (Kanai *et al*., 1992). Alterations in the phosphorylation state of tau, notably hyperphosphorylation, have been implicated in the formation of paired helical filaments (PHFs), which are integral components of NFT and may precede their assembly into PHF (Bancher *et al*., 1989). In addition, hyperphosphorylated tau loses its ability to bind to microtubules, leading to a disruption in microtubule assembly and deficits in axonal transport (see review by Mi and Johnson (2006)). Given clinical evidence showing a correlation between NFT density and disease progression (Braak and Braak, 1991; Arriagada *et al*., 1992), and recent studies reporting age-dependent synaptic deficits, hippocampal degeneration and memory impairment in transgenic mice overexpressing mutant forms of tau (Ramsden *et al*., 2005; Yoshiyama *et al*., 2007), strategies targeting tau pathology are attractive for the treatment of AD.

Tau is encoded by a single gene located on chromosome 17 and alternative splicing leads to the formation of six

Correspondence: Dr J Lotharius, Department of Molecular Biology, H Lundbeck A/S, Ottiliavej 9, 2500 Valby, Copenhagen, Denmark.
E-mail: mjl@lundbeck.com

isoforms, all of which can be found in the adult brain (Goedert *et al.*, 1998; Hong *et al.*, 1998). Phosphorylation of tau by several kinases, including mitogen-activated protein kinase (MAPK), cyclin-dependent kinase 2/5 (CDK2/5), and glycogen synthase kinase-3β (GSK-3β) generates epitopes found in AD brains (Drewes *et al.*, 1992; Baumann *et al.*, 1993; Mandelkow *et al.*, 1995). GSK-3 is a serine/threonine kinase known to phosphorylate several substrates and involved in diverse cellular pathways such as cell signalling and survival. Two related isoforms, GSK-3α and β, are expressed in the adult mammalian brain and share similarities in their catalytic domains and substrate specificity (Woodgett, 1990, 1991; Plyte *et al.*, 1992). GSK-3α/β are regulated at multiple levels by post-translational phosphorylation of $Ser^{21/9}$ (inhibitory) and $Tyr^{279/216}$ (activating) by interaction with docking proteins such as axin and presenilins that bring together the enzyme and its priming kinase (for example, casein kinase and protein kinase A) and by intracellular distribution (Van and Haefner, 2003; Kockeritz *et al.*, 2006).

Recent studies have explored the involvement of GSK-3β in abnormal tau phosphorylation, NFT formation and APP processing (Pei *et al.*, 1999; Ferrer *et al.*, 2005). GSK-3β phosphorylates sites corresponding to PHF-tau including Ser^{202}, Ser^{396}, Thr^{181} and Thr^{231} according to the longest human tau isoform containing 441 residues (Goedert *et al.*, 1989; Hanger *et al.*, 1998). In early AD, active GSK-3β has been associated with pre-PHF/tangles (Yamaguchi *et al.*, 1991; Pei *et al.*, 1999). Additional observations showing increased expression of GSK-3β in post-synaptosomal compartments in affected brain regions (Pei *et al.*, 1997) and decreased activity and levels of protein phosphatases A/B (PP-2A/B) in AD (Gong *et al.*, 1995, 2000; Vogelsberg-Ragaglia *et al.*, 2001; Rahman *et al.*, 2005), suggest that a combined dysregulation in both pathways could contribute to enhanced tau phosphorylation in the disease.

During recent years, distinct classes of small-molecule GSK-3 inhibitors have been developed for various conditions including diabetes, mood disorders and AD (Meijer *et al.*, 2004; Huang and Klein, 2006). LiCl and AR-A014418, a thiazole class inhibitor, were shown to reduce insoluble, hyperphosphorylated tau in the brainstem of JNPL3 transgenic mice overexpressing a mutant form of human tau (Noble *et al.*, 2005). Aminopyrimidine derivatives, originally developed for diabetes, showed efficacy in lowering the blood glucose levels in rodent disease models (Ring *et al.*, 2003). Although many *in vitro* studies have examined the effect of GSK-3 inhibitors on phosphorylated tau (p-tau) levels, neuroprotection (Hoeflich *et al.*, 2000; Bhat *et al.*, 2003) and amyloid-β (Aβ) production (Phiel *et al.*, 2003), very little is known about their effect on disease-related end points *in vivo*.

In the current study, we used a postnatal rat model characterized by high levels of p-tau linked to enhanced GSK-3β activity (Takahashi *et al.*, 1995; Leroy and Brion, 1999), to evaluate the effect of pharmacological inhibition of GSK-3 on this pathological hallmark of AD and correlated it to enzyme activity *ex vivo*, inhibition of recombinant GSK-3β and to its effect on kinase activity and p-tau in a human neuronal cell line.

Methods

Animals

All animal procedures were performed in accordance with the guidelines of the Danish National Committee on Animal Research Ethics and the European Communities Council Directive no. 86/609 for the Care of Laboratory Animals.

Time-mated female Wistar rats were ordered from Harlan, The Netherlands. Rats taken at postnatal days 0–28 (P0-28), as well as 3-month-old rats, were killed by decapitation for establishment of the postnatal rat model; postnatal day 12 pups (P12) were used for inhibitor efficacy studies.

Immunohistochemical analysis

P12 and adult rats were anaesthetized with tribromoethanol (4 mg per 100 g body weight) intraperitoneally (i.p.) and perfused with 4% phosphate-buffered paraformaldehyde via the ascending aorta. Brains were post-fixed with in the same fixative for 4 h at room temperature (RT) and cryoprotected in 30% sucrose in phosphate-buffered saline (PBS). Brains were cut into 40 μm cryosections. For long-term storage, sections were transferred to cryoprotectant and kept at −20 °C. To quench endogenous peroxidase activity, sections were treated with 1% H_2O_2 and then blocked with 5% normal porcine serum in PBS/1% bovine serum albumin (BSA)/0.3% Triton X-100. The sections were incubated at 4 °C overnight with 1:100 monoclonal mouse anti-p-tau antibody (clone AT8; Innogenetics, Alpharetta, Georgia, USA) in PBS/1% BSA/0.3% Triton X-100. Sections were then rinsed 3×10 min in PBS and incubated for 60 min with a biotinylated horse anti-mouse antibody diluted 1:500 (Dako, Glostrup, Denmark). The sections were rinsed again and incubated with the avidin–biotin complex (no. PK 6100, Vector, Burlingame, CA, USA) at RT for 60 min. After rinsing, the sections were reacted with 0.05% 3,3′-diaminobenzidine (DAB) in 0.01% H_2O_2 in PBS for 5–20 min. After staining, images were captured with a JenOptik ProgRes digital camera and analysed using an Openlab imaging station (Improvision, Coventry, UK). Density slicing of regions of interest under standardized conditions was used to detect the area of staining (staining index).

Preparation of brain tissue extracts

For investigation of p-tau levels during rat brain postnatal development (postnatal day 0 to adulthood) brain tissue was homogenized as described previously (Mawal-Dewan *et al.*, 1994) with some minor modifications. Briefly, tissue was diluted 1.5-fold w v^{-1} of buffer A (100 mM 2-(*N*-morpholino) ethanesulphonic acid (MES), pH 6.5, 0.5 mM magnesium acetate, 1 mM EGTA, 5 mM 2-mercaptoethanol, 0.1 mM phenylmethylsulphonyl fluoride, 1 μg ml^{-1} pepstatin and 1 μg ml^{-1} leupeptin) and centrifuged at 50 000 *g* for 30 min at 2 °C. The supernatant was collected and centrifuged again at 115 000 *g* for 70 min at 2 °C. This final supernatant was used to investigate p-tau levels by western blotting as described in the following section.

After timed administration of GSK-3 inhibitors, P12 rats were killed and the brain removed. Half of the brain was used

for brain exposure studies and the other half was dissected on ice to separate the hippocampus and cortex for western blotting and GSK-3β activity assays. Tissue was stored at −80 °C until processed. For western blot analysis, crude brain homogenates were prepared by sonicating tissue on ice in 50 mM Tris-HCl, 150 mM NaCl, 1% Triton X-100, 1 mM NaF and 2 mM Na_3VO_4 and 1 × Complete protease inhibitor cocktail (Roche, Denmark) and centrifuging at 18 000 *g* for 15 min at 4 °C. Pellets were discarded and protein concentration in the supernatant determined using the bicinchoninic acid (BCA) protein determination kit from Pierce, Herlev, Denmark.

For GSK-3β activity assays, the cortex from P12 animals treated with different GSK-3 inhibitors was homogenized in ice-cold radioimmunoprecipitation assay (RIPA) buffer containing 50 mM Tris-HCl, 1% nonidet P-40 (NP-40), 150 mM NaCl, 1 mM EDTA, pH 7.4 with 0.25% Na-deoxycholate, 1 mM NaF, 1 mM Na_3VO_4, 1 mM 4-(2-aminoethyl) benzene sulphonyl fluoride hydrochloride (AEBSF) and 1 × Complete protease inhibitor cocktail for 30 min on ice. The tissue was centrifuged at 18 000 *g* for 15 min at 4 °C. The supernatant was then collected and the protein concentration of the lysate measured using the BCA protein assay.

Western blotting

Briefly, brain homogenates were prepared as described previously and 10 μg of protein containing 4 × LDS (lithium dodecyl sulphate) loading buffer, was heated to 60 °C for 5 min and proteins separated by electrophoresis on 4–12% Bis–Tris NuPage gels using sodium dodecyl sulphate (SDS)-MOPS ((3-(*N*-morpholino) propane sulphonic acid) running buffer. A SeeBlue pre-stained molecular mass marker (Invitrogen, Taastrup, Denmark) was run on each gel for protein size determination. Proteins were separated at 150 V for 2 h and subsequently transferred onto 0.45 μm polyvinylidene difluoride (PVDF) membranes at 40 V for 2 h. The membranes were blocked for 1 h at RT using 5% non-fat dry milk in 20 mM Tris buffer, pH 7.6, with 137 mM NaCl and 0.05% (w v^{-1}) Tween-20. Subsequently, membranes were incubated with primary antibody in blocking buffer overnight at 4 °C. Monoclonal antibodies recognizing distinct phosphorylated epitopes of p-tau and total tau (both phosphorylated and non-phosphorylated forms) were used. The antibodies corresponding to different epitopes of human tau were used at the following dilutions: Ser^{396} (1:5000), AT-8, recognizing Ser^{202}/Thr^{205} (1:1000), AT270, recognizing Thr^{181}, (1:4000) and tau 5, recognizing total tau, (1:5000). A monoclonal mouse antibody to glyceraldehyde-3-phosphate dehydrogenase (GAPDH) (1:5000) was used as a loading control. Membranes were washed three times with 20 mM Tris buffer, pH 7.6, with 137 mM NaCl and 0.05% (w v^{-1}) Tween-20 and incubated with a secondary horseradish peroxidase (HRP)-labelled goat antibody against rabbit IgG (1:1000) or a rabbit antibody against mouse IgG (1:2000) for 1 h at RT. After an additional washing step, immunolabelled proteins were visualized using chemiluminescence (ECL plus, Amersham, Birkerod, Denmark). Blots were stripped with 20 mM Tris, pH 7.2, 10% SDS and 100 mM β-mercaptoethanol and reprobed with anti-GAPDH to normalize for amount of protein loaded. Western blots were scanned using a FujiFilm LAS300 Intelligent Dark Box scanner, and the band density of each blot was quantified within the linear range of detection using the FluoroChem 8800 system and AlphaEase software.

Immunoprecipitation-based method for measuring GSK-3β activity in cells

A human immortalized cell line that can be differentiated into neuronal-like cells, LUHMES (Lotharius *et al*, 2002, 2005), was used to measure the effect of various inhibitors on GSK-3β enzyme activity. Cells were treated with six concentrations (ranging from 0.001 to 100 μM) of the following: SB216763, TDZD-8, Alsterpaullone, Indirubin-3′-monoxime, CHIR98014 and AR-A014418 (all dissolved in dimethylsulphoxide (DMSO), which was used for as a vehicle-treated control) for 6 h at 37 °C and then lysed with ice-cold RIPA buffer (50 mM Tris-HCl, 1% NP-40, 150 mM NaCl, 1 mM EDTA, pH 7.4) containing 0.25% Na-deoxycholate, 1 mM NaF, 1 mM Na_3VO_4, 1 mM AEBSF and 1 × Complete protease inhibitor cocktail for 30 min on ice. The supernatant was collected, and the protein concentration was measured using the BCA protein determination assay. For immunoprecipitation of GSK-3β, 50 μl of DYNA beads were rinsed three times with PBS/0.1% BSA and re-suspended in 10 μl PBS/0.1% BSA. GSK-3β was purified by adding 5 μl of 250 μg ml^{-1} purified monoclonal mouse anti-GSK-3β antibody. The samples were incubated for 1 h at 4 °C and rinsed three times in PBS/0.1% BSA. The antibody-labelled beads were re-suspended in 50 μl of cell extraction buffer (10 mM Tris-HCl pH 7.4, 50 mM NaCl, 1 mM EGTA, 1 mM EDTA, 50 mM β-glycerophosphate, 3 mM benzamidine, and 0.05% NaN_3, 50 mM NaF, 100 μM Na_3VO_4 and 1 mM AEBSF) after which 10 μg of LUHMES cell lysate was added to the mixture and incubated for 1 h at 4 °C. The immune complex was then rinsed three times in cell extraction buffer and two more times in assay buffer (50 mM HEPES, 10 mM $MgCl_2$, 5 mM $MnCl_2$, 1 mM DTT, 1 μM ATP). The enzyme reaction was performed by incubating the immunoprecipitates in assay buffer (see above) containing 5 μg phospho-glycogen synthase (GS) peptide-2 and 20 μCi [γ-^{33}P]ATP for 30 min at 30 °C. Both a positive (recombinant GSK-3β) and a negative control (reaction mixture with no protein or reaction containing 2 μM CHIR98014) were performed for every experiment. The reaction was stopped by the addition of 4 × LDS loading buffer containing 1% β-mercaptoethanol. Samples were then boiled at 95 °C for 5 min and proteins separated by SDS-polyacrylamide gel electrophoresis (PAGE) on 16% Tricine-SDS-polyacrylamide gels (Invitrogen). Gels were stained with Coomassie blue and autoradiographed. Incorporation of ^{33}P into GS peptide after 30 min by GSK-3β immunoprecipitated from 10 μg total cellular protein was measured by densitometry (AlphaEase FluoroChem 8800 software). IC_{50} values were calculated using sigmoidal dose–response curve fit analysis.

Immunoprecipitation-based method for measuring GSK-3β activity in tissue extracts

This assay was performed as described above with a few modifications: 1.5 μg of cortical tissue homogenized in

ice-cold RIPA buffer was added to the beads and incubated for 1 h at 4 °C. The immune complex was rinsed three times in cell extraction buffer and two more times in assay buffer. The immunoprecipitates were then incubated in assay buffer including containing 5 μg GS peptide-2, 1 μCi [γ-^{33}P]ATP for 15 min at 30 °C. A positive and negative control was also performed for every experiment. The remainder of the procedure is performed as described above. Incorporation of ^{33}P into GS peptide after 15 min by GSK-3β immunoprecipitated from 1.5 μg total cellular protein was measured by densitometry (AlphaEase FluoroChem 8800 software) and expressed as percent inhibition compared to vehicle-treated controls.

Recombinant GSK-3β activity assay

GSK-3β activity was measured using FLASH-plates (PerkinElmer Life Science, Waltham, Massachusetts, USA) pre-coated with streptavidin and a biotin-labelled GS peptide as substrate (biotin-(EACA)PRPASVPPSPSLSRHSSPHQS(PO_3H_2)EDEE-NH_2, Schafer-N, Denmark). Human recombinant GSK-3β was provided by Dundee University (Dundee, UK). Following the GSK-3β-catalysed transfer of the ^{33}P from [γ-^{33}P]ATP (Amersham) to the substrate, the proximity of ^{33}P-substrate to the scintillation-coated well results in a detectable signal. The assay was performed in 100 μl total volume of assay buffer containing 12 mM MOPS, 10 mM Mg-acetate, 0.2 mM EDTA, and 1 mM dithioerythritol (DTE), pH 6.6 and the following: the test compound, 2 μCi ml^{-1} ATP, 0.1 μM substrate and 30 mU ml^{-1} enzyme incubated for 1 h at RT. Washing two times with 100 μl PBS terminated the reaction and the plates were subsequently counted in a Wallac Microbeta counter (PerkinElmer Life Sciences, USA). Background was defined by including 10 μM staurosporine, and the IC_{50} values were calculated by nonlinear regression fit using the Levenburg Marquardt algorithm of the data to the four-parameter logistic function: $y = A + ((B-A)/(1 + ((Cx^{-1})^D)))$, where A denotes the bottom plateau of the curve, B the top of the plateau of the curve, C the log EC_{50} and D the slope factor.

Drugs and drug administration

SB216763 (30 mg kg^{-1}) and CHIR98014 (30 mg kg^{-1}) were resuspended in DMSO and injected i.v. AR-A014418 (30 mg kg^{-1}), was dissolved in 100% PEG400 and administered *per os* (p.o.) Indirubin-3′-monoxime (20 mg kg^{-1}) and Alsterpaullone (20 mg kg^{-1}) were dissolved in 20% DMSO/25% Tween-80 and injected i.p. and s.c., respectively. All drug studies were conducted using P12 rats from the same litter. Control animals were dosed with the respective vehicle and both groups were killed after 1, 2 and 4 h for brain exposure measurements (see the next section), western blotting and GSK-3β activity assays. Experiments measuring the efficacy of each compound were performed at least three times and at a time point determined by brain exposure data.

LiCl (100 and 200 mg kg^{-1}) was dissolved in sterile water, and administered p.o. to animals. P12 rats were killed 8 h after injection. Some of the littermates were used as the control group and dosed with NaCl (100 or 200 mg kg^{-1}, p.o.) dissolved in sterile water.

Brain exposure measurements

Rat brain homogenates were analysed for exposure levels of SB216763, Indirubin-3′-monoxime, Alsterpaullone, CHIR98014 and AR-A014418 using turbulent flow chromatography (HTLC) followed by detection by Tandem mass spectrometry (MS/MS). Four times 70% v w^{-1}acetonitrile was added to the sample and homogenized in an autogizer robot (Tomtech, Hamden, CT, USA). The brain homogenate was centrifuged at 6000 *g* for 15 min at 5 °C, and the supernatant was analysed. Calibration curves (1–1000 ng ml^{-1} brain homogenate) for each compound were prepared using brain homogenate from untreated rats. A total of 25 μl of 10% MeOH with internal standard (citalopram) was added to either 25 μl of brain homogenate or calibration standard, followed by centrifugation at 6000 *g* for 20 min at 5 °C). Ten microlitres of each sample was injected into the HTLC system using a HTS PAL autosampler (Cohesive Technologies, Franklin, MA, USA). Samples with AR-A014418 were purified using 0.1% HCOOH in water for 15 s (2 ml min^{-1}) using a Cyclone HTLC column (0.5 × 50 mm, 50 μm, Cohesive Technologies). The compounds were extracted from the HTLC using 100 μl 0.1% HCOOH/90% acetonitrile placed in the loop and transferred to the analytical column, X-Terra MS C_8 (20 × 2.1 mm, 3.5 μm, Waters, Milford, MA, USA) with 0.1% HCOOH in water over 120 s (0.08 ml min^{-1}) and eluted from the analytical column using a gradient from 0.1% HCOOH/2% MeCN to 0.1% HCOOH/98% acetonitrile for 45 s, followed by elution with 0.1% HCOOH/98% acetonitrile for 120 s flow 0.5 ml min^{-1}). Detection of the compound was performed using Ultima triple-quadropole mass spectrometer (Waters) and positive ionization using multiple reaction monitoring set at optimal conditions. For AR-A014418 the transition 308.9 → 121.7 was used.

All other samples were purified using 0.1% NH_3OH/5% MeOH (2.25 ml min^{-1}) for 45 s using a Cyclone HTLC column (0.5 × 50 mm, 50 μM, Cohesive Technologies). The compounds were extracted from the HTLC column using 100 μl 90% MeOH placed in the loop and transferred to the analytical column, X-Terra MS C8 (20 × 2.1 mm, 3.5 μM, Waters) with 0.1% NH_3OH in water over 120 s (0.08 ml min^{-1}) and eluted from the analytical column using a gradient from 0.1% NH_3OH/2% MeOH to 0.1% NH_3OH/98% MeOH for 105 s, followed by elution with 0.1% NH_3OH/98% MeOH for 120 s (flow 0.35 ml min^{-1}). Detection of the compounds was performed using a Sciex API3000 triple–quadruple mass spectrometer (Applied Biosystems, Foster City, CA, USA). Alsterpaullone was analysed using negative ionization and SB216763, Indirubin-3′-monoxime and CHIR98014 were analysed using positive ionization electrospray with multiple-reaction monitoring set at optimal conditions for each compound. The following transitions were used: CHIR98014 (4859 → 164.1), SB216763 (371.0 → 336.3) and Indirubin-3′-monoxime (278.0 → 259.9), Alsterpaullone (294.8 → 226.8). Values represent atomic mass units.

The concentration of the compounds in brain homogenates was determined by standard calibration curve analysis, using linear fitting of a $1/x$-weighted plot of the compound/internal standard peak area ratios vs compound concentration.

LUHMES experiments

A human immortalized cell line that can be differentiated into neuronal-like cells, LUHMES (Lotharius *et al*., 2002, 2005), was used to measure the effect of various GSK-3 inhibitors on tau phosphorylation, GSK3β activity and cell death. LUHMES cells were grown as described previously (Lotharius *et al*., 2002), and treated after 4 days of differentiation with 2 μM GSK-3 inhibitors for 6 h and Ser^{396} tau phosphorylation measured using a human Ser^{396} p-tau ELISA kit (BioSource International, Camarillo, CA, USA) after lysis as per the manufacturer's instructions. Data are standardized to protein concentration and expressed as percent inhibition of p-tau compared to vehicle-treated control; in this case DMSO. To determine the neuroprotective effect of GSK-3 inhibitors used in this study, differentiated LUHMES cells were co-treated with 2 μM of each compound together with the phosphatidyl-inositol 3 (PI3) kinase inhibitor, LY294002, used at 50 μM. After 72 h, cell death was assessed using the (3-(4,5-dimethylthiazol-2-yl)-2,5-diphenyltetrazolium bromide (MTT) reduction assay. Data are presented as percent inhibition against LY294002 toxicity compared to vehicle-treated controls.

Statistical analysis

Data were analysed by two-tailed Student's *t*-test for the LiCl study (two groups). One-way analysis of variance (ANOVA) was used to analyse the data from the studies with the rest of the inhibitors (three or more groups). Values in graphs from *in vivo* studies are expressed as mean ± s.d.

Antibodies and chemicals

Monoclonal antibodies used for western blotting were purchased from the following manufacturers: rabbit polyclonal anti-Ser^{396} p-tau antibody and mouse monoclonal anti-tau antibody (clone tau-5) from BioSource/Invitrogen; mouse monoclonal anti-human PHF-tau antibody (clone AT-8) from Innogenetics, Zwijnaarde, Belgium; mouse monoclonal anti-human PHF-tau antibody (clone AT270) from Pierce Biotechnology, Rockford, IL, USA; monoclonal mouse anti-GSK-3β antibody from BD Bioscience, San Jose, CA, USA; and anti-mouse monoclonal GAPDH antibody (clone no. mAbcam 9484) from Abcam, Cambridge, UK. HRP-labelled goat anti-mouse and anti-rabbit antibodies were purchased from Dako. Other chemicals used for western blotting were purchased from Invitrogen. For immunoprecipitation of GSK-3β and enzyme activity assays, chemicals used were as follows: DYNA beads (rat anti-mouse IgG1) from DYNAL Biotech ASA (Oslo, Norway); phospho-GS peptide-2 from Upstate Biotechnology, UK; and [γ-^{33}P]ATP from Amersham.

The drugs used in this study were purchased from the following manufacturers: SB216763 from Tocris Cookson Ltd, Bristol, UK; Indirubin-3′-monoxime from Sigma, Brondby, Denmark; and Alsterpaullone from Calbiochem, Darmstadt, Germany. CHIR98014 (Chiron Corporation/Novartis AG; WO-0996589) and AR-A014418 (AstraZeneca AB, Bhat *et al*., 2003) were re-synthesized at H Lundbeck A/S, according to published methods. The PI3 kinase inhibitor, LY294002, was from Cayman Chemical (Ann Arbor, Mi, USA). Ser^{396} p-tau kit was purchased from BioSource International. All other chemicals were purchased from Sigma.

Results

Tau is hyperphosphorylated during early postnatal development in the rat

Previous studies (Takahashi *et al*., 1995; Leroy and Brion, 1999) have shown an increase in p-tau and elevated GSK-3β protein and activity levels in the developing rodent brain, which peaked at postnatal day 12 (P12). To correlate these findings with the ultimate goal of establishing a model for testing the *in vivo* efficacy of GSK-3 inhibitors on tau phosphorylation, we used the AT8 antibody recognizing Ser^{202}/Thr^{205} p-tau to examine the pattern of tau phosphorylation throughout different stages of development in the rat brain. Whereas most areas in the adult brain, including the hippocampus (Hip), exhibited weak p-tau staining, strong immunoreactivity was present in some regions, including the hypothalamus and piriform (Pir) cortex (Figure 1a). In contrast, an intense immunostaining was observed throughout the P12 brain (Figure 1b). In the adult hippocampus, weak p-tau immunoreactivity was mainly localized to pyramidal and granular somata (Figure 1c), whereas somata as well as axonal and dendritic compartments were clearly immunostained in the P12 hippocampus (Figure 1d). In cortical regions, neuronal perikarya and apical dendrites were weakly p-tau positive in the adult rat (Figure 1e) in contrast to equivalent sections from P12 rat brain, where somata and neurites were strongly stained (Figure 1f). The overall p-tau staining pattern, or staining index, was quantified by 'density slicing' of the dentate gyrus as described in the Methods section and found to be significantly increased (Figure 1g). P12 brains stained with the Ser^{396} antibody showed the same p-tau immunoreactivity pattern as the regions processed with AT8 (data not shown). Neither P12 nor adult rat brains were stained and analysed for the levels of total tau (phosphorylated and unphosphorylated forms), which could have been done using a tau 5 antibody. Studies investigating the distribution of tau during development using anti-total tau antibodies (Brion *et al*., 1994; Takahashi *et al*., 2000) showed staining in neurons and proximal neurites in the neocortex and hippocampus of 9-day-old rats. The staining intensity in the cell soma and apical dendrites appeared to be increased in 5-week-old rats. This differed from the staining pattern seen, which was weaker, when using phospho-specific antibodies. Also, as demonstrated by our western blotting analyses (see Figures 2b, c and f) no change in the levels of total tau was observed in cortex or hippocampus of 11-day-old pups and adult rats.

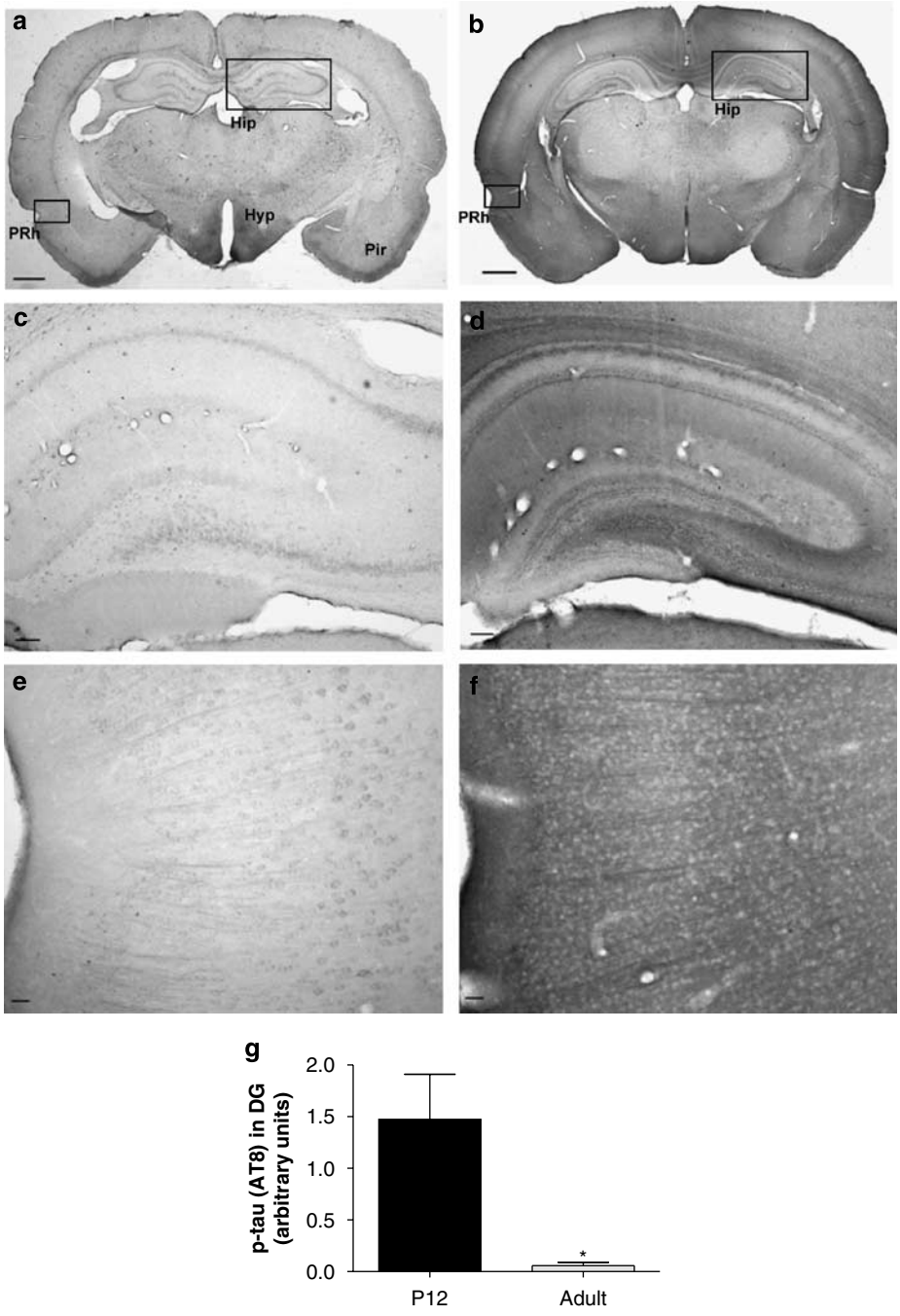

Figure 1 Localization of p-tau in the postnatal and adult rat brain. Coronal sections from rat brain were immunostained with an AT8 (1:1000) antibody recognizing Ser^{202}/Thr^{205} phosphorylated epitopes of tau. Immunoreactivity for p-tau was prominent throughout (**b**) the P12 brain compared to the adult (**a**), where strong immunostaining was present in piriform cortex (Pir) and areas of hypothalamus (Hyp). (**c**) In adult hippocampus (Hip) somata were weakly immunoreactive whereas (**d**) cell bodies and neuronal processes were strongly labelled in the P12 hippocampus. (**e**) p-tau immunoreactivity could be observed in neuronal perikarya and apical dendrites in adult cortical regions (perirhinal cortex, PRh). (**b** and **f**) In P12, somata and neuropil showed intense staining throughout cortical regions. (**g**) Quantification of the staining index in dentate gyrus (DG) was performed by density slicing as described in the Methods section (*$P<0.05$, *t*-test followed by Mann–Whitney, $n=3$). Scale bars: (**a** and **b**) = 1 mm; (**c** and **d**) = 100 μm; (**e** and **f**) = 25 μm. p-tau, phosphorylated tau.

To support these immunohistochemical findings, the levels of p-tau were examined by western blot analysis using several antibodies recognizing different epitopes of p-tau: AT8, Ser^{396} and AT270. Studies were performed in whole brain (Figures 2a and b), cortex (Figures 2c and d) and hippocampus (Figures 2e and f) from animals killed 0, 7, 9, 11, 17, 21, 23, 26 and 28 days after birth (postnatal days 0–28; P0-28) and compared with the corresponding adult brain regions. SDS-PAGE investigation of tissue from different brain regions showed the appearance of four distinct tau bands in adult tissue samples ranging from 43 to 56 kDa. The bands are likely to represent four of the six isoforms of tau

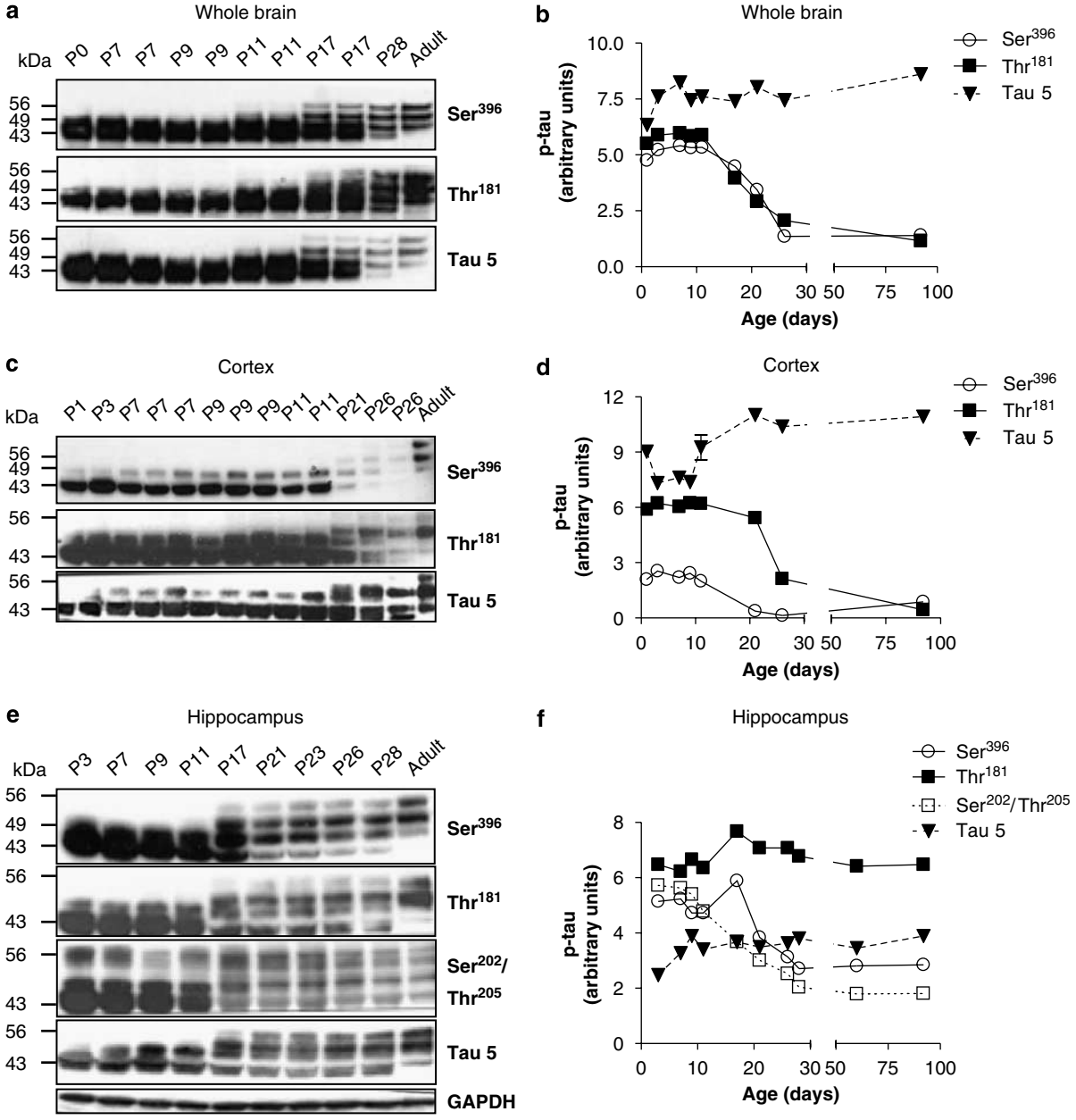

Figure 2 Characterization of the postnatal rat model. Levels of p-tau during early postnatal development (P0-P11) were compared to those of older (P17-adult) rats by western blot analysis using Ser^{396}, Thr^{181} and Ser^{202}/Thr^{205} p-tau-specific antibodies recognizing phosphorylated epitopes that overlap with PHF-p-tau. Western blot analysis of whole brain (**a**), cortex (**c**) and hippocampus (**e**), shows two major bands during postnatal development migrating at 43 and 49 kDa, probably to represent the two major isoforms of fetal tau. Adult tau constitutes at least four isoforms/bands on SDS-PAGE, the largest isoform detected being 56 kDa. Ser^{396} and Thr^{181} p-tau were quantified in whole brain (**b**), cortex (**d**) and Ser^{396}, Thr^{181} and Ser^{202}/Thr^{205} p-tau were quantified in hippocampus (**f**), throughout postnatal development. (**a**, **c** and **e**) the level of total tau (as detected with a tau 5-specific antibody) was also monitored during development. Band densities were quantified within the linear range of detection using the FluoroChem 8800 system and AlphaEase software after scanning blots with a Fuji Film LAS300 light box. GAPDH was used as a loading control. Quantification was performed using densitometry analysis and values shown represent mean $\pm$ s.d. GAPDH, glyceraldehyde-3-phosphate dehydrogenase; PHF, paired helical filament; p-tau, phosphorylated tau; SDS-PAGE, sodium dodecyl sulphate-polyacrylamide gel electrophoresis.

known to arise from alternative splicing of exons 2, 3 and 10 and inclusion of N-terminal inserts (Goedert *et al.*, 1998; Hong *et al.*, 1998).

In juvenile brain tissue two main bands were visible, namely a 43 and a 49 kDa band, which as suggested by a previous report, may correspond to 3R0N and 4R0N tau, respectively (Brandt and Leschik, 2004; Figures 2a, c and e). Densitometry analysis of tau isoforms during postnatal development in whole brain, cortex and hippocampus showed an increase in juvenile p-tau levels during P0-11, peaking at P11 and a subsequent decrease of these forms starting at P17 until adulthood (Figures 2b, d and f). In contrast, the predominantly adult isoform of tau, likely represented by the 56-kDa band, appeared at P17 and

continued to increase in intensity into adulthood in all tissues investigated (Figures 2a, c and e). As shown previously, this isoform is expressed late in rodent development (Brandt, 1996) as corroborated by our model. Since a similar increase in p-tau levels was observed with different antibodies recognizing several epitopes of p-tau such as AT8 and AT270 as with the Ser^{396} antibody, and phosphorylation of the latter epitope is clearly involved in PHF formation and microtubule destabilization (Bramblett *et al*., 1993), we decided to use the Ser^{396} antibody during the continuation of our study. Finally, analysis of total tau (phosphorylated and unphosphorylated forms) as detected by a tau 5 antibody showed a stable 25% increase of total tau during postnatal development (>P3) and adulthood when compared to P0 in both whole brain and hippocampal tissue. In cortex, a slightly smaller increase was seen (≈20%), following a transient ≈20% decrease in total tau between P3 and P11 (Figure 2d). This is in contrast to previous reports (Mawal-Dewan *et al*., 1994; Takahashi *et al*., 1995) claiming that total tau, which was measured by a phosphorylation independent antibody, increases from P9 into adulthood in all three tissue samples.

We then investigated the activity levels of GSK-3β in our system using an immunoprecipitation-based assay modified from that of Planel *et al*. (2001) as described in the Methods section. Basal enzyme activity levels were analysed in whole brain, cortical and hippocampal tissue from P12 rats and adult rats. Total GSK-3β enzyme activity was measured by incorporation of ^{33}P into the GS peptide by GSK-3β isolated from 1.5 μg protein. As reported previously (Takahashi *et al*., 1995; Leroy and Brion, 1999), GSK-3β enzyme activity was significantly higher in P12 than in adult rats: 36% in whole brain (Figures 3a and d), 44% in cortex (Figures 3b and e) and 55% in hippocampus (Figures 3c and f).

In conclusion, we have carefully characterized the pattern of tau phosphorylation in a postnatal rat model using various antibodies corresponding to epitopes present in PHF-tau and show that hyperphosphorylation of tau in cortex, hippocampus and whole brain tissue takes place in early postnatal development in the rat and correlates with increased GSK-3β enzyme activity.

Lithium chloride reduces tau phosphorylation in postnatal rats

The effects of LiCl, an ATP non-competitive inhibitor of GSK-3 (Jope, 2003; Phiel*et al*., 2003) (IC_{50} = 1–2 mM), has been tested in various *in vitro* neuronal systems (Hong *et al*., 1997; Munoz-Montano *et al*., 1997). *In vivo*, chronic LiCl administration was shown to reduce the aggregation of P301L mutant tau linked to fronto-temporal dementia linked to chromosome 17 (FTDP-17) in a transgenic mouse model (Perez *et al*., 2003). Nevertheless, taking in account the many potential targets of LiCl, the need for pharmacological tools is important.

In this study, we wanted to confirm the ability of LiCl to reduce tau phosphorylation *in vivo* by using the postnatal rat model. For this purpose, P12 rats were dosed with 100 mg kg^{-1} LiCl for 8 h and compared to NaCl-treated animals. The levels of p-tau in cortical tissue were analysed by western blotting using the Ser^{396} antibody. Treatment of P12 rats with LiCl resulted in a fourfold decrease in the phosphorylation of both 43 and 49 kDa tau bands, respectively in the cortex when quantified by densitometry (Figures 4a–c). In addition, the lowering effect of LiCl was observed when using AT8 and AT270 (data not shown) antibodies suggesting that the effect of lithium is not epitope-specific. The effect was dose dependent, with no change in p-tau observed at 50 mg kg^{-1} using the full antibody panel (data not shown). Thus, we decided to continue our study using only one of the antibodies; in this case Ser^{396}. P-tau as detected with this antibody will be referred to as 'p-tau' in the following sections. Hippocampal P12 rat tissue was investigated in a similar manner as described above revealing a significant decrease in the phosphorylation of the 43 kDa band by lithium but no change in the 49 kDa band when analysed by western blotting (Figures 4d–f).

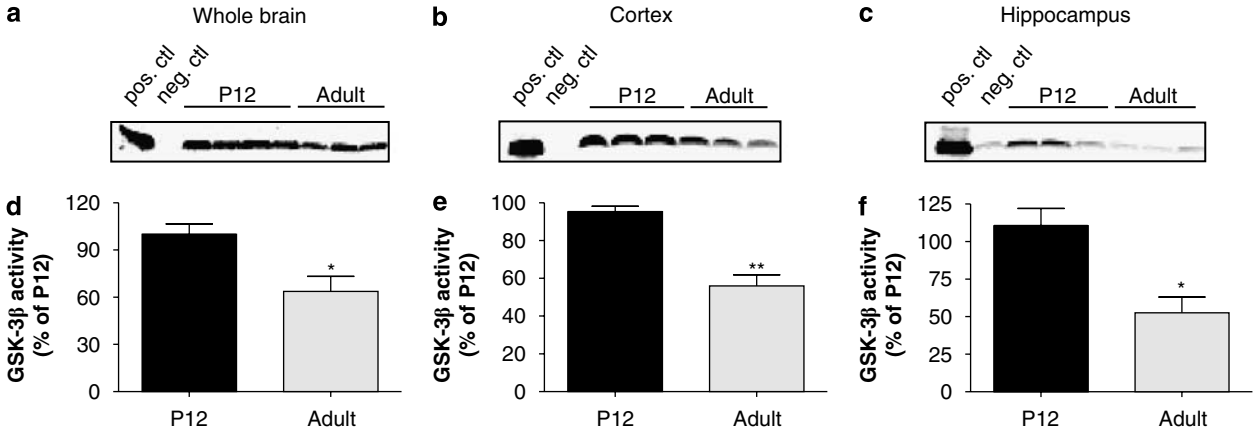

Figure 3 GSK-3β enzyme activity was increased in postnatal rats. (**a**) GSK-3β enzyme activity was assessed by measuring the incorporation of [γ-^{33}P]ATP into a synthetic GS peptide as described in the Methods section. Lysates from (**a**) whole brain, (**b**) cortex and (**c**) hippocampus from P12 vs adult animals were compared for enzyme activity levels. (**d**, **e** and **f**) Quantification was performed using densitometry analysis of autoradiographic film. Data are expressed as percentage of enzyme activity of P12 tissue and represent mean ± s.d. (n = 3–4, *P < 0.05, **P < 0.01, Student's t-test). GS, glycogen synthase; GSK-3β, glycogen synthase kinase-3β.

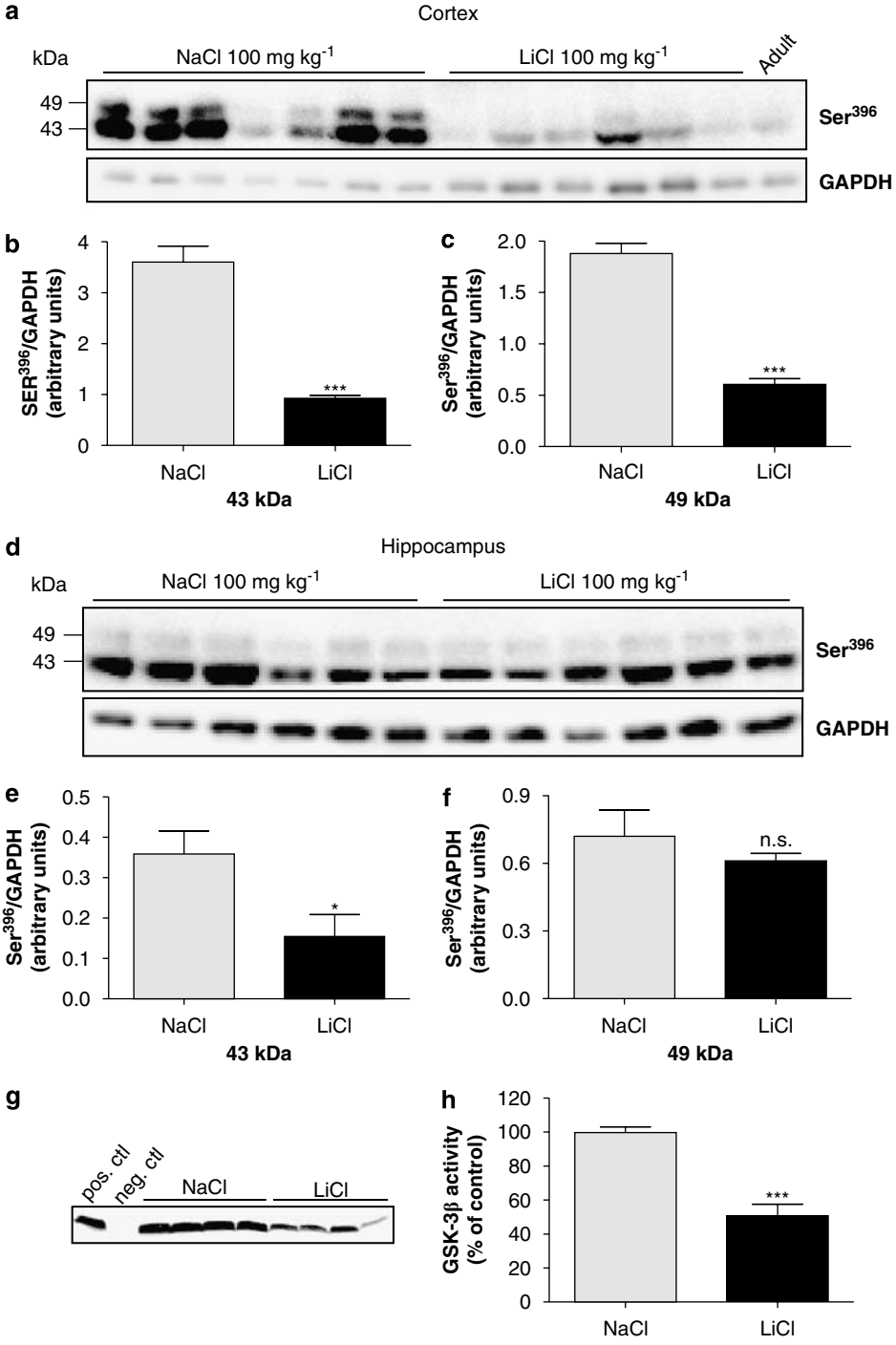

Figure 4 Lithium chloride reduced tau phosphorylation *in vivo*. Animals were given 100 mg kg^{-1} LiCl (dissolved in sterile water) p.o. for 8 h and (**a**) cortical tissue was analysed by western blotting using a Ser^{396} p-tau-specific antibody (1:5000). (**b**) Both 43 kDa and (**c**) 49 kDa bands were quantified by densitometry. Data are expressed as Ser^{396} p-tau normalized to GAPDH and represent the mean ± s.d. (***$P<0.005$, *t*-test followed by Mann–Whitney test, $n=6$). (**d**) Western blotting of hippocampus was analysed as described above. (**e** and **f**) The effect of LiCl on p-tau levels was quantified by densitometry of both 43 and 49 kDa bands and compared to NaCl-treated animals. Data represent mean ± s.d. and are expressed as Ser^{396} p-tau normalized to GAPDH (*$P<0.05$, *t*-test followed by Mann–Whitney test, $n=6$). (**g**) Total GSK-3β enzyme activity was measured in cortical tissue lysates of P12 animals treated with 100 mg kg^{-1} lithium chloride, p.o., for 8 h (*$P<0.05$, $P<0.05$, *t*-test followed by Mann–Whitney test, $n=6$). (**h**) Quantification of ^{33}P incorporated into a GS peptide was by densitometric analysis of autoradiographic film. Data are expressed as percentage of enzyme activity of NaCl-treated animals and represent mean ± s.d. ($n=4$, ***$P<0.005$, Student's *t*-test). GAPDH, glyceraldehyde-3-phosphate dehydrogenase; GS, glycogen synthase; p-tau, phosphorylated tau.

To confirm that the reduction of p-tau by LiCl was indeed correlated to its inhibition of GSK-3β (Phiel and Klein, 2001), the activity of this enzyme was investigated in cortical tissue from P12 rats treated for 8 h with 100 mg kg^{-1} LiCl or the same dose of NaCl. Total GSK-3β enzyme activity was measured, as described earlier in cortical tissue lysates. A

35% decrease in enzyme activity was seen when compared to vehicle-treated animals demonstrating that the effect of lithium treatment on p-tau levels is directly linked to inhibition of GSK-3β (Figures 4g and e). It is unlikely that lithium, being a reversible inhibitor of GSK-3β (Stambolic *et al*., 1996), remains bound to the enzyme after the immunoprecipitation procedure explaining the observed decrease in kinase activity. Both *in vivo* and *in vitro* studies have shown an increase in Ser^{9} phosphorylation in cortical neurons following LiCl treatment (De Sarno *et al*., 2002), an epiphenomenon that could be responsible for the lower GSK-3 enzyme activity levels seen in the *ex vivo* assay. Indeed, Ser^{9} phosphorylation after lithium treatment was also seen in the current study (data not shown).

Various classes of GSK-3 inhibitors reduce tau phosphorylation in the postnatal rat

To our knowledge, attempts to demonstrate the *in vivo* efficacy of the majority of GSK-3 inhibitors have not been undertaken or published. Furthermore, since there is limited published data on the efficacy of these inhibitors in reducing tau phosphorylation *in vivo* and *in vitro*, we chose to test a battery of GSK-3 inhibitors belonging to distinct chemical classes in our postnatal rat as well as in a human, neuronal *in vitro* model. The IC_{50} of these compounds was also determined using recombinant GSK-3β and in a cell-based neuronal system to obtain an idea of membrane permeability (see the next section).

Before *in vivo* administration, the solubility properties of each inhibitor were assessed based on chemical structure, and different vehicles chosen using this information (Table 1). To achieve the highest accumulation of drug in the brain various doses and routes of administration were tested as described in the Methods section. Using turbulent flow chromatography (HTLC) followed by detection by MS/MS, we monitored the brain levels of each compound at different time points after drug administration. Here we present experimental data where the maximal conditions (brain concentration and effect on tau phosphorylation) for each compound were achieved.

Thiazole. AR-A014418 has been reported to reduce p-tau levels in JNPL3 mice (Noble *et al*., 2005) and was therefore tested in our model. AR-A014418 was dissolved in polyethylene glycol 400 (PEG 400) and injected $30\,mg\,kg^{-1}$ p.o. for 2, 4 and 6 h. After 2 h of drug administration $\approx 3\,\mu M$ of AR-A014418 could be detected in whole brain homogenates, which decreased to 1.2 μM after 4 h (Table 1). Surprisingly, no effect of the compound on the phosphorylation levels of either 43 or 49 kDa tau could be observed in the cortex or hippocampus at any time point studied (see Table 1; only data for 4 h time point shown (Figures 5a–f). Furthermore, a slight but not significant effect of the vehicle used, PEG-400, on hippocampal p-tau levels was observed when compared to naive animals. We also tested the effect of AR-A014418 dissolved in 25% Cremaphor EL at $10\,mg\,kg^{-1}$, given s.c. The concentration of this compound measured in the whole brain after 2 h was $\approx 0.5\,\mu M$, a concentration sixfold lower than that obtained at the same time point when PEG-400 was used. Western blotting analysis using the same epitope-specific antibody of tissue extracted 2, 4 and 6 h after drug exposure showed no effect on p-tau levels in the cortex or hippocampus. The different doses and vehicles used for this compound are also summarized in Table 1. AR-A014418 also failed to show an effect on tau phosphorylation in LUHMES cells when used at 2 μM, a concentration well above its IC_{50} of 300 nM (Table 2).

Bis-Indole. We chose to continue testing another GSK-3 inhibitor, Indirubin-3′-monoxime, which has shown *in vitro* effects on tau phosphorylation (Leclerc *et al*., 2001). Similar to AR-A014418, Indirubin-3′-monoxime, injected $20\,mg\,kg^{-1}$, i.p., did not affect p-tau levels in either the cortex or hippocampus of P12 rats despite the high concentration of the compound in the brain (13 μM; Table 1) and a low IC_{50} (26 nM; Table 2). Indirubin-3′-monoxime induced a 30–45% reduction in 43 and 49 kDa hippocampal p-tau isoforms when compared to naive animals, but this modest vehicle effect was not statistically significant (one-way ANOVA). In addition, there was no change in either the 43 or 49 kDa p-tau bands after 2 h (cortex) and 1 h (hippocampus) between drug and vehicle-treated groups, as shown in Figures 6a–f. Despite our efforts to optimize delivery by using different routes of administration or vehicles, we did not succeed in observing an effect of this compound on p-tau levels in the P12 rat brain (Table 1). Notably, Indirubin-3′-monoxime was difficult to dissolve in various vehicles tested and correspondingly very low brain levels were often observed in such vehicles (Table 1). Interestingly, while having no effect in the postnatal rat model, Indirubin-3′-monoxime reduced p-tau levels in neuronal cultures (see below), a discrepancy that could be explained by high protein binding or increased metabolism *in vivo*.

Aminopyrimidine. The novel GSK-3 inhibitor CHIR98014, which has been thus far only tested in rodent models of diabetes, displayed an $IC_{50} = 4$ nM in a recombinant enzyme activity assay (see below) and was very potent at decreasing Ser^{396} tau phosphorylation in a human neuronal cell line, LUHMES, when used at 2 μM (Table 2). This prompted us to test its effect on tau phosphorylation *in vivo*. P12 rats were injected i.v. with $30\,mg\,kg^{-1}$ of the compound dissolved in DMSO. Different doses, vehicles and routes of administration were tested and brain exposure studies were performed (see Methods section and Table 1). Dissolving the compound in DMSO and injecting it i.v. led to a maximal concentration in the brain of 7 μM (Table 2). Animals were therefore treated i.v. with $30\,mg\,kg^{-1}$ CHIR98014 for 1, 2 and 4 h. As shown in Table 1, accumulation of CHIR98014 in the brain reached a peak after 1 h and remained stable even after 2 and 4 h of injection. Tissue analysed by western blotting using a Ser^{396} p-tau antibody showed a $\approx 40\%$ reduction in the phosphorylation of 43 and 49 kDa tau in the cortex (Figures 7a–c). A significant, threefold reduction in the 43 kDa isoform was also observed in the hippocampus (Figures 7d and e), while no significant reduction in 49 kDa was observed at any time point (Figures 7d and f). Furthermore, a dose-dependent decrease in p-tau levels was also observed when CHIR98014

Table 1 Brain levels and routes of administration for various classes of GSK-3 inhibitors investigated in the postnatal rat model

Inhibitor	*Class*	*Vehicle*	*Dose and route of administration*	*Brain levels (μM)*	*% p-tau inhibition in cortex*	*% p-tau inhibition in hippocampus*
Lithium chloride	Ion	NaCl	p.o. (100 mg kg^{-1})	ND	75% (43 kDa) 60% (49 kDa)	50% (43 kDa) NC (49 kDa)
			p.o. (200 mg kg^{-1})	ND	58% (43 kDa) 30% (49 kDa)	48% (43 kDa) 34% (49 kDa)
SB216763 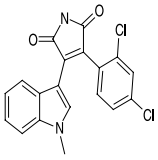	Arylindolemaleimide	10% DMSO/ 90% PEG400	p.o. (10 mg kg^{-1})	0.07 (1 h) 0.1 (4 h)	50% (43 kDa) NC	NC 50% (43 kDa)
			i.p. (30 mg kg^{-1})	0.2 (2 h)	NC	NC
		10% cyclodextrin DMSO	i.v. (30 mg kg^{-1})	15 (2 h)	NC	50% (43 + 49 kDa)
		10% DMSO/ 90% PEG400	p.o. (30 mg kg^{-1})	0.1 (1 h, 2 h)	NC	NC
		DMSO	i.v. (30 mg kg^{-1})	2.5 (2 h)	NC	30–58% (43 + 49 kDa)
AR-A014418 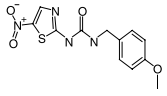	Thiazole	100% PEG400	p.o. (30 mg kg^{-1})	3 (2 h) 2 (4 h) 0.8 (6 h)	NC NC NC	NC NC NC
		25% Cremaphor EL	s.c. (10 mg kg^{-1})	0.5 (2 h) 1.2 (4 h) 0.8 (6 h)	NC NC NC	NC NC
Indirubin-3′-monoxime 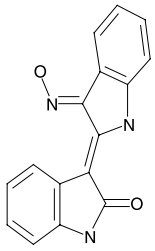	Bis-Indole	10% cyclodextrin	i.p. (50 mg kg^{-1})	0.01–0.6 (1 h)	NC	NC
		20% DMSO/25% Tween-80	i.p. (20 mg kg^{-1})	13 (1 h), 8 (2 h), 2 (4 h)	NC	NC
		DMSO	i.v. (30 mg kg^{-1})	17 (1 h), 12 (2 h), 0.5 (4 h)	NC	NC
Alsterpaullone 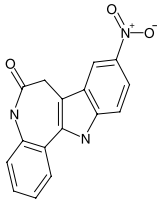	Benzazepinone	20% DMSO/ 25% Tween-80	i.p. (10 mg kg^{-1})	ND (4 h) nd (1 h)	26% (43 kDa) NC (49 kDa) NC	NC 48% (43 kDa)
		DMSO	i.v. (30 mg kg^{-1})	2.5 (2 h)	NC	34% (49 kDa)
		20% DMSO/ 25% Tween-80	s.c. (20 mg kg^{-1})	0.35 (2 h)	20% (43 kDa) NC (49 kDa)	NC 50% (43 kDa) NC (49 kDa)
CHIR98014 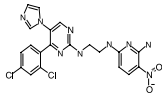	Aminopyrimidine	15% captisol	s.c. (30 mg kg^{-1})	(1 h)	NC	NC
			i.p. (30 mg kg^{-1})	(2 h)	NC	NC
		10% cyclodextrin	(60 mg kg^{-1})	0.1 (1 h)	NC	NC
		DMSO	i.v. (30 mg kg^{-1})	7 (1 h)	45% (43 kDa) 42% (49 kDa)	67% (43 kDa) NC (49 kDa)

Abbreviations: DMSO, dimethylsulphoxide; NC, no change; ND, not detectablein the brain following MS/MS; p-tau, phosphorylated tau.
The chemical structure and class of each inhibitor are shown. The concentration of each compound detected in the brain by turbulent flow chromatography (HTLC) followed by detection by Tandem mass spectrometry (MS/MS) is expressed in micromolar units at a time point where the highest concentration in the brain was observed (shown in brackets; time points for lithium are not given). The dose (mg kg^{-1}), vehicle, and time points used are presented. For each compound, the observed decrease in Ser^{396} p-tau levels (of both the 43 and 49 kDa bands) is shown as the % reduction compared to their respective vehicles.

was injected i.v. for 1 h at different doses (1–30 mg kg^{-1}) although a significant reduction was only detectable at doses above 10 mg kg^{-1} (Figures 8a–c). The potency of CHIR98014 correlated well with its maximal brain concentration (7 μM) and IC_{50} for this compound (3.7 nM, Table 2). At 2 μM, CHIR98014 led to a >90% reduction in p-tau in a human neuronal cell line (Table 2).

To explore whether the mechanism underlying the observed decrease in tau phosphorylation was directly linked to the selectivity of CHIR98014 towards GSK-3β, we

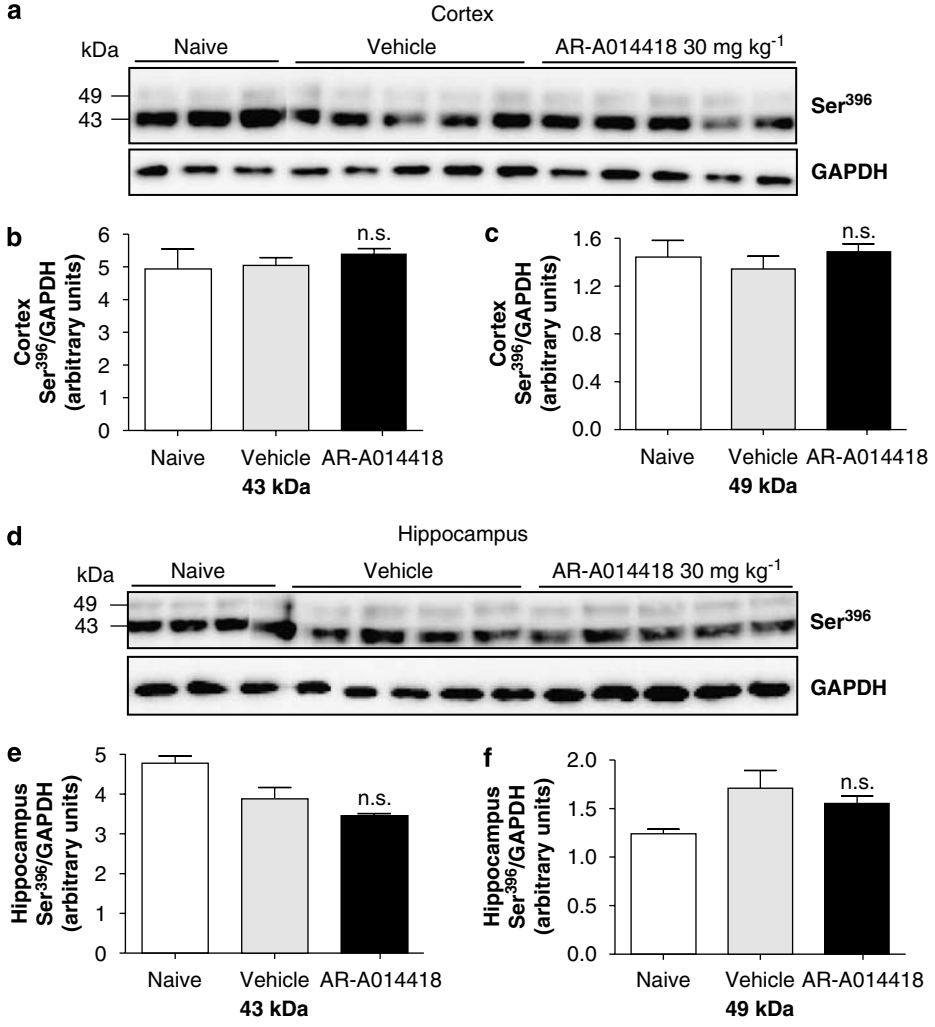

Figure 5 The thiazole GSK-3 inhibitor, AR-A014418, did not affect tau phosphorylation *in vivo*. (**a**) Levels of 43 and 49 kDa Ser^{396} p-tau were quantified by western blotting in cortical lysates of P12 rats given 30 mg kg^{-1} AR-A014418 (dissolved in 100% PEG 400 and administered p.o.) for 4 h. (**b**) Both 43 kDa and (**c**) 49 kDa bands were quantified by densitometry (NS, $P>0.05$, compared to vehicle, one-way ANOVA followed by Dunnett's test $n=5$). (**d**) Western blotting of hippocampus were analysed as described above. (**e** and **f**) The effect of 30 mg kg^{-1} AR-A014418 (4 h administration) on p-tau levels was quantified by densitometry of both 43 and 49 kDa bands and compared to vehicle-treated animals. Data represent mean ± s.d. and are expressed as Ser^{396} p-tau normalized to GAPDH (NS, $P>0.05$, compared to vehicle, one-way ANOVA followed by Dunnett's test, $n=5$). ANOVA, analysis of variance; GAPDH, glyceraldehyde-3-phosphate dehydrogenase; GSK-3, glycogen synthase kinase-3; p-tau, phosphorylated tau.

measured the activity of this kinase in homogenates of cortical tissue taken from P12 rats 1 h after injection i.v. with CHIR98014 (30 mg kg^{-1}). A 50% reduction in GSK-3β activity levels was observed in CHIR98014-treated animals compared to vehicle-treated rats (Figures 7g and h). Control experiments showed that at peak brain concentrations, CHIR98014 did not remain bound to the enzyme during the immunoprecipitation procedure and the observed decrease in enzyme activity could, as in the case of lithium, be due to autoinhibitory phosphorylation at the Ser^{9} epitope (data not shown).

Arylindolemaleimide. Similar to CHIR98014, the GSK-3 inhibitor SB216763 also decreased p-tau levels in our neuronal cultures and exhibited an IC_{50} in the 10 nM range, which prompted us to test it in the postnatal rat model for an *in vivo* effect. The highest levels were obtained in whole brain homogenates when the compound was dissolved in DMSO and injected i.v. to P12 rats (15 μM at 2 h; Table 1). Thus, P12 rats were injected i.v. with 30 mg kg^{-1} SB216763 dissolved in DMSO, and the levels of p-tau in drug- vs vehicle-treated animals were assessed after 2 h by western blotting. Even though no decrease in tau phosphorylation was observed in the cortex at this time point (Figures 9a–c), SB216763 showed a consistent reduction in the phosphorylation of both 43 and 49 kDa p-tau in the hippocampus compared to vehicle-treated animals (Figures 9d–f). In addition, a significant increase in the phosphorylation state of 49 kDa tau was observed in cortical tissue from animals treated with SB216763 as compared to naive animals with a small yet nonsignificant vehicle effect seen between the vehicle and naive groups (Figures 9a and c). Since all compound effects were compared to vehicle-treated rats and no statistical difference was seen between SB216763 and vehicle-treated

Table 2 *In vitro* data for different classes of GSK-3 inhibitors including effects on enzyme activity, p-tau reduction and neuroprotection in LUHMES cells

Inhibitor	*Recombinant GSK-3β assay IC_{50} [nM], Reference*	*Recombinant GSK-3β assay IC_{50} [nM], Selenica et al*	*Cell-based GSK-3β assay IC_{50} [nM]*	*Max brain concentration [nM]*	*% inhibition p-tau at 2 μM, LUHMES*	*% inhibition LY294002 toxicity at 2 μM, LUHMES*
AR-A014418	104 Bhat *et al.* (2003)	300	16200	2000	0	31
SB216763	34 Coghlan *et al.* (2000)	9.2	150	15000	41	46
TDZD-8	2000 Martinez *et al.* (2002)	>10000	9727	ND	0	3
Indirubin-3′-monoxime	22 Leclerc *et al.* (2001)	26	236	13000	54	68
Alsterpaullone	4 Leost *et al.* 2000	15	62	350	62	51
CHIR98014	0.63 Ring *et al.* (2003)	3.7	70	7000	93	52

Abbreviations: DMSO, dimethylsulphoxide; GS, glycogen synthase; GSK-3, glycogen synthase kinase-3; MTT, (3-(4,5-dimethylthiazol-2-yl)-2,5-diphenyltetrazolium bromide.
The IC_{50} for each compound was determined by the incorporation of ^{33}P into a GS peptide by human recombinant GSK-3β. The incorporated radioactivity was measured via scintillation and IC_{50} values calculated by nonlinear regression. Data are shown in [nM]. For the cell-based GSK-3β activity assay, LUHMES cells were treated with GSK-3 inhibitors for 6 h and GSK-3β activity measured, as described in Methods section. Densitometry analysis was performed on autoradiographic film and IC_{50}s calculated using sigmoidal dose-response curve fit analysis. Data are shown in [nM]. For determination of tau phosphorylation, LUHMES cells were treated for 6 h with 2 μM inhibitors, lysed, and human, endogenous Ser^{396} p-tau levels measured using an ELISA kit from Biosource. Data are shown as percentage inhibition of Ser^{396} p-tau compared to DMSO-treated cells. For neuroprotection experiments, LUHMES cells were co-treated with 2 μM inhibitors and 50 μM of the PI3 kinase inhibitor, LY294002, for 72 h and cell viability measured using the MTT reduction assay. Data are shown as % inhibition of LY294002-induced toxicity compared to DMSO-treated controls.

rats, we did not explore this phenomenon further. Interestingly, in the hippocampus, the opposite effect was observed, that is a decrease in p-tau levels induced by the vehicle, in comparison to naive animals, and a smaller, yet significant effect when comparing SB216763 to vehicle-treated controls (Figures 9d–f).

The disparity between the p-tau levels in cortex and hippocampus led us to investigate GSK-3β enzyme activity levels in both brain regions after drug exposure (Figures 9g–j). Cortical and hippocampal tissue from P12 rats injected i.v. with SB216763 (30 mg kg^{-1}) for 2 h was homogenized, and the GSK-3β activity were measured. A 60% reduction in GSK-3β activity levels was observed in the hippocampus but not cortex of SB216763-treated animals compared to vehicle-treated rats. Again, the reduction in kinase activity seen in the *ex vivo* assay is likely to reflect enhanced Ser^9 phosphorylation following inhibition of the enzyme, as shown by a recent study (Liang and Chuang, 2006).

Benzazepinone. Next, we investigated the effect of Alsterpaullone in the postnatal rat model. Data in neuronal cultures showed a positive effect on p-tau at 2 μM, a concentration >100 times higher than its IC_{50} (Table 2). This inhibitor was dissolved in several vehicles and given by various routes of administration. Even though a maximal concentration of 2.5 μM achieved after 2 h when the drug was given i.v., this approach did not lead to a reduction in p-tau levels in either cortex or hippocampus (Table 1). However, dissolving the compound in 20% DMSO/25% Tween-80 and injecting it s.c. at a dose of 20 mg kg^{-1}, resulted in a brain concentration of 350 nM (Table 1) and led to a reduction in 43 kDa tau phosphorylation in cortex after 2 h, as shown in Figures 10a–c. No change in the 49-kDa isoform was observed. In hippocampus, the phosphorylation levels of 43 and 49 kDa isoforms were significantly decreased when analysed 2 h after drug administration (Figures 10d–f). It is noteworthy to mention that we also observed a small albeit not significant effect of the vehicle on p-tau levels (49 kDa isoform) as compared to naive animals in this experimental set-up.

Determination of IC_{50} values for various GSK-3 inhibitors

The enzyme IC_{50} values for different GSK-3 inhibitors were determined by utilizing the [γ-^{33}P]ATP-streptavidin-FLASH-plate assay, described in the Methods section. From the IC_{50} values shown in Table 2, we found the following rank order of potency: CHIR98014 > SB216763 > Alsterpaullone > Indirubin-3′-monoxime > AR-A014418 > TDZD-8. In accordance with the published values, the aminopyrimidine class of inhibitor, CHIR98014, was shown to be the most potent compound with an IC_{50} of 3.7 nM (the published IC_{50} is 0.63 nM; Ring *et al.*, 2003).

The apparent K_m value for ATP was determined by measuring the amount of phosphorylated substrate under conditions with a constant [γ-^{33}P]ATP concentration (2 μCi ml^{-1}) and increasing concentrations of unlabelled ATP at different time points from 10 to 60 min. Values are given as mean with (min; max) values, because of the logarithmic distribution of the IC_{50} and apparent K_m. Linearity in product formation over time was observed under all conditions tested. These experiments showed a

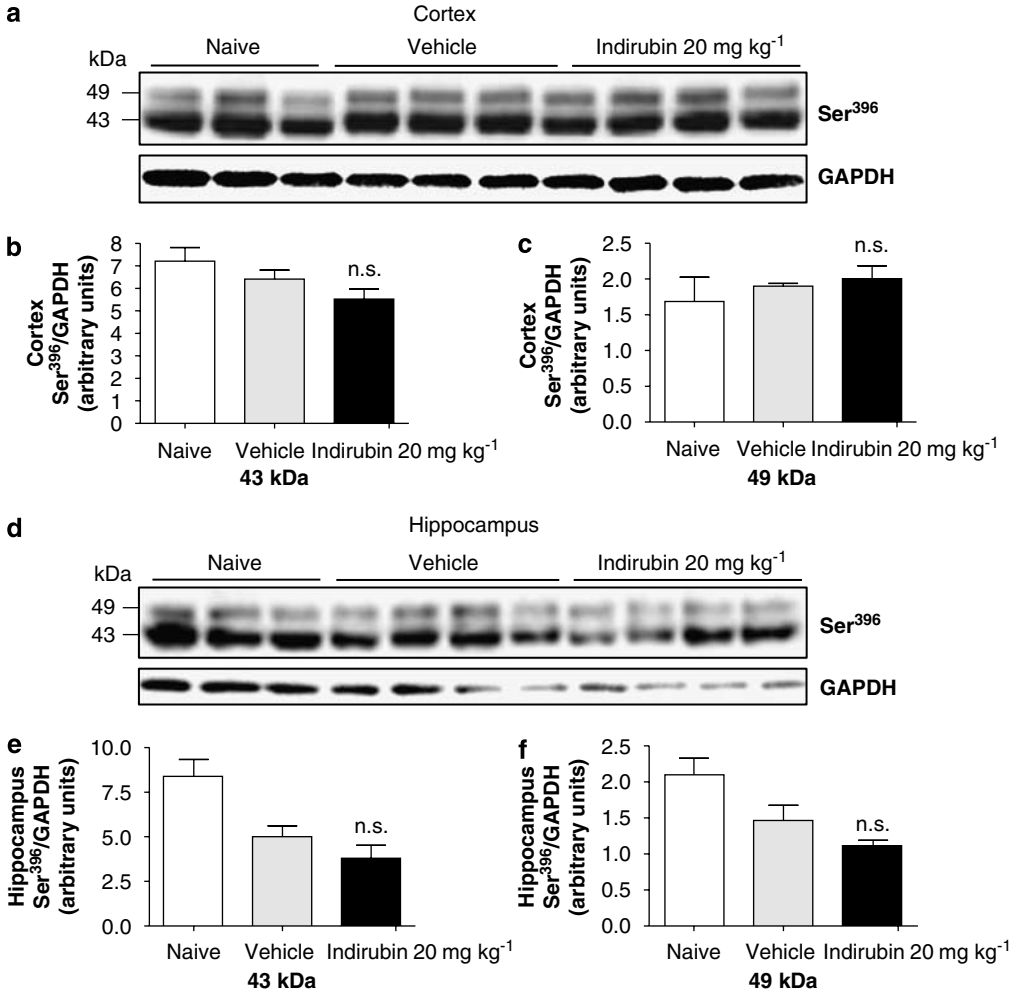

Figure 6 The bis-indole GSK-3 inhibitor, Indirubin-3′-monoxime, did not reduce tau phosphorylation *in vivo*. (**a**) Levels of 43 and 49 kDa Ser^{396} p-tau were quantified by western blotting in cortical lysates of P12 rats given 20 mg kg^{-1} Indirubin-3′-monoxime for 2 h. (**b**) Both 43 kDa and (**c**) 49 kDa bands were quantified by densitometry (NS, $P>0.05$, compared to vehicle, one-way ANOVA followed by Dunnett's test $n=5$). (**d**) Western blotting of hippocampus analysed as described above. (**e** and **f**) The effect of 20 mg kg^{-1} Indirubin-3′-monoxime (1 h administration) on p-tau levels was quantified by densitometry of both 43 and 49 kDa bands and compared to vehicle-treated animals. Data represent mean ± s.d. and are expressed as Ser^{396} p-tau normalized to GAPDH (NS, $P>0.05$, compared to vehicle, one-way ANOVA followed by Dunnett's test, $n=5$). ANOVA, analysis of variance; GAPDH, glyceraldehyde-3-phosphate dehydrogenase; GSK-3, glycogen synthase kinase-3; p-tau, phosphorylated tau.

time independent apparent K_m for ATP ranging from 0.6 to 1.9 μM over time with an average of 0.86 μM (0.74 μM; 1.00 μM, $n=6$). All inhibitor experiments were performed under conditions with only labelled [γ-^{33}P]ATP present in the reaction, hence at ATP concentrations well below the K_m value. At this low ATP concentration, the IC_{50} value of staurosporine was not affected by changes in [γ-^{33}P]ATP concentration, as the IC_{50} value was unchanged over a 100-fold range of [γ-^{33}P]ATP from 0.2 to 20 μCi ml^{-1}. At 2 μCi ml^{-1} the IC_{50} value for staurosporine was determined to be 2.1 nM (1.3 nM; 3.4 nM, $n=8$). Half-maximal inhibition experiments with a number of known GSK-3 inhibitors were performed under the conditions described above and all but TDZD-8 showed concentration-dependent inhibition with IC_{50} values ranging from 4 to 300 nM (Table 2). TDZD-8 did not result in any significant inhibition at concentrations up to 10 μM. This discrepancy with previous published results (Martinez *et al*., 2002) can most probably be ascribed to the differences in assay conditions. Martinez *et al*. (2002) determined the IC_{50} value of TDZD-8 as 2 μM.

For the cell-based assay, differentiated LUHMES cells were treated with increasing concentrations of various GSK-3 inhibitors for 6 h, and the total enzyme activity was measured. The resulting IC_{50} values for most of the inhibitors were 4- to 20-fold higher than those determined in the recombinant GSK-3β assay, with the exception of AR-A014418, which was 50-fold higher, and TDZD-8, which showed an IC_{50} of ≈10 μM in both analyses (Table 2). This is most probably ascribed to the differences in assay conditions, such as concentration of substrate or radioactive ATP used. In addition, the discrepancy between the recombinant IC_{50} values and those obtained in the cell-based LUHMES assay could be explained by differences in membrane permeability for each inhibitor, degradation in the medium or following cellular uptake, or increased p-glycoprotein-mediated cellular efflux of compounds that are substrates for this transporter.

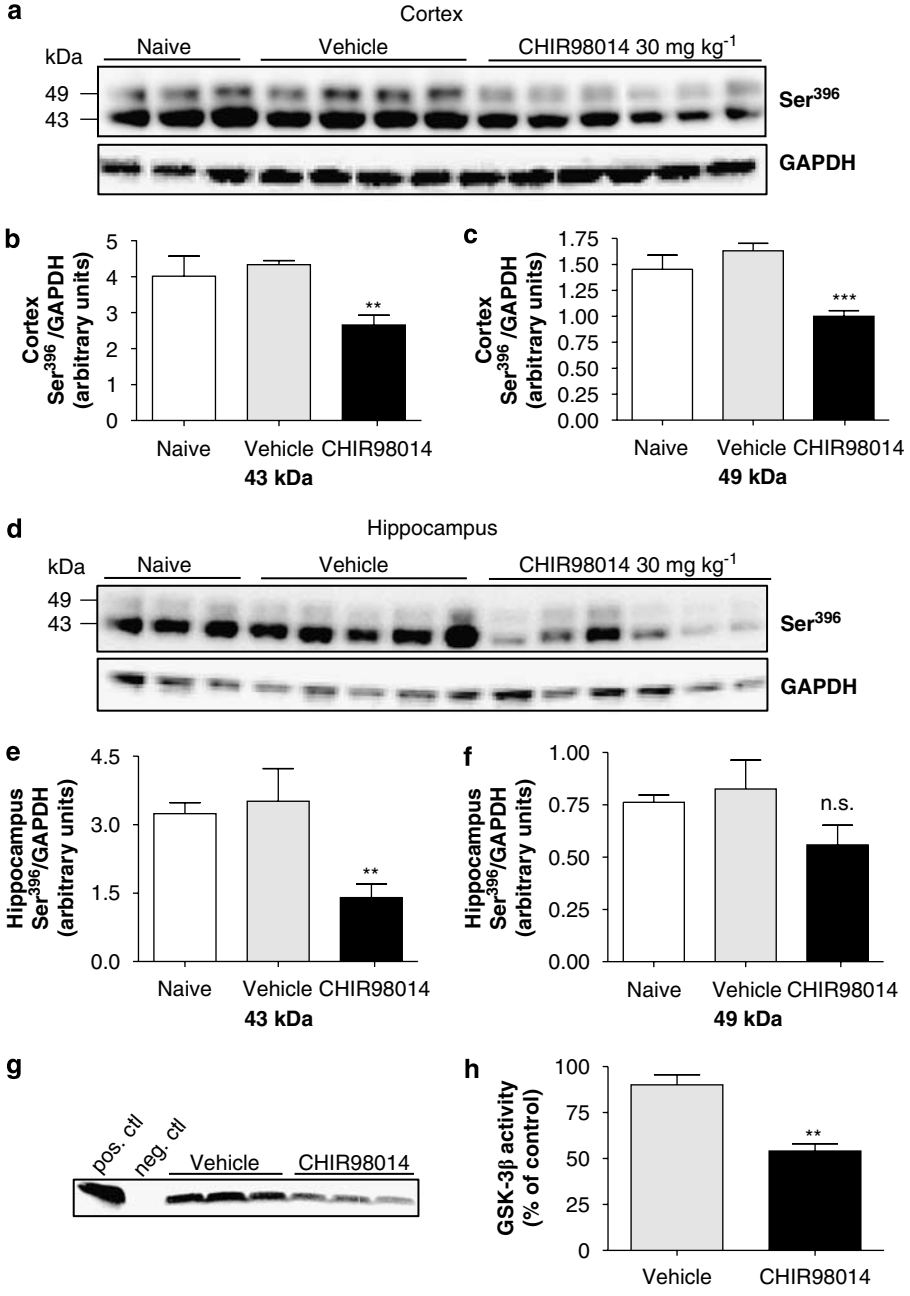

Figure 7 The aminopyrimidine GSK-3 inhibitor, CHIR98014, reduced tau phosphorylation *in vivo*. P12 rats were given 30 mg kg^{-1} CHIR98014 (dissolved in sterile DMSO) i.v. and (**a**) p-tau levels in the postnatal rat cortex were analysed by western blotting using a Ser^{396} antibody (1:5000). (**b** and **c**) 43 and 49 kDa p-tau levels in the cortex were quantified by densitometry and compared to vehicle-treated animals. Data represent mean ± s.d. and are expressed as Ser^{396} p-tau normalized to GAPDH (***$P<0.001$, **$P<0.01$, compared to vehicle, one-way ANOVA followed by Dunnett's test; $n=6$). (**d**) Western blotting of hippocampal tissue from rats given 30 mg kg^{-1} CHIR98014 i.v. was performed and p-tau levels quantified by densitometry of both 43 and 49 kDa bands and compared to DMSO-treated animals as shown in (**e** and **f**). Data represent mean ± s.d. and are expressed as Ser^{396} p-tau normalized to GAPDH (**$P<0.01$, NS $P>0.05$, compared to vehicle, one-way ANOVA followed by Dunnett's test; $n=6$). (**g**) Total GSK-3β enzyme activity was measured in cortical lysates of P12 rats treated with 30 mg kg^{-1} CHIR98014, i.v. for 1 h. (**h**) Incorporation of ^{33}P into a GS peptide was quantified by densitometry analysis of autoradiographic film. Data are expressed as percentage of enzyme activity compared to vehicle-treated animals and represent the mean ± s.d. (**$P<0.01$, *t*-test followed by Mann–Whitney test, $n=3$). ANOVA, analysis of variance; DMSO, dimethylsulphoxide; GAPDH, glyceraldehyde-3-phosphate dehydrogenase; GS, glycogen synthase; GSK-3, glycogen synthase kinase-3; p-tau, phosphorylated tau.

All GSK-3 inhibitors were also tested for their efficacy in inhibiting endogenous tau phosphorylation at the Ser^{396} epitope in LUHMES cells, Differentiated LUHMES cells were treated for 6 h with different classes of GSK-3 inhibitors used at a concentration of 2 μM and the levels of Ser^{396} p-tau determined by ELISA. Most of the inhibitors tested significantly lowered p-tau levels in intact cells when used at a concentration of 2 μM, with the exception of TDZD-8 and AR-A014418 (Table 2). Interestingly, despite its IC_{50} values in both the recombinant and cell-based assay and its ability to

lower p-tau in LUHMES cells, Indirubin-3′-monoxime was not efficacious in lowering p-tau *in vivo*.

Lastly, the ability of these inhibitors to block LUHMES cell death induced by LY294002, a specific PI3 kinase inhibitor, shown to activate GSK-3β by inhibiting Akt-mediated Ser^{9} (autoinhibitory) phosphorylation of the enzyme (Vlahos *et al.*, 1994), was tested in parallel cultures. Cells were co-treated with 2 μM of each GSK-3 inhibitor and 50 μM LY294002 and cell survival monitored after 72 h using the MTT reduction assay. CHIR98014, Alsterpaullone and Indirubin-3′-monoxime were the most efficacious at rescuing cells from LY294002-induced cell death at this concentration, showing >50% neuroprotection, followed closely by SB216763 (Table 2). These data correlated well with the IC_{50} obtained in the LUHMES assay, which ranged from 70 to 236 nM (Table 2). Furthermore, the ability of these inhibitors to decrease p-tau levels correlated with their neuroprotective potential suggesting that both tau phosphorylation and LY294002 toxicity are mediated by GSK-3β. Compounds largely ineffective at reducing p-tau and LY294002-induced toxicity at 2 μM (for example, AR-A014418 > TDZD-8) displayed cell-based IC_{50}s in the 9–16 μM range.

Discussion

The correlation between high levels of p-tau and GSK-3β activity observed in juvenile rat brains (Takahashi *et al.*, 1995; Leroy and Brion, 1999) suggests that GSK-3β is involved in tau hyperphosphorylation during brain development (Takahashi *et al.*, 1995). In fact, GSK-3β immunoreactivity has been colocalized with p-tau in hippocampal CA3 pyramidal neurons in the P12 rat brain (Takahashi *et al.*, 2000). We confirmed an elevation in p-tau in the cerebral cortex, hippocampus and whole brain during postnatal development in rats by using several antibodies recognizing AD-relevant epitopes of p-tau including Ser^{202}, Ser^{396} and Thr^{205}. By western blotting, we showed that the phosphorylation of both 43 and 49 kDa band tau isoforms were dramatically increased compared to adults. In addition,

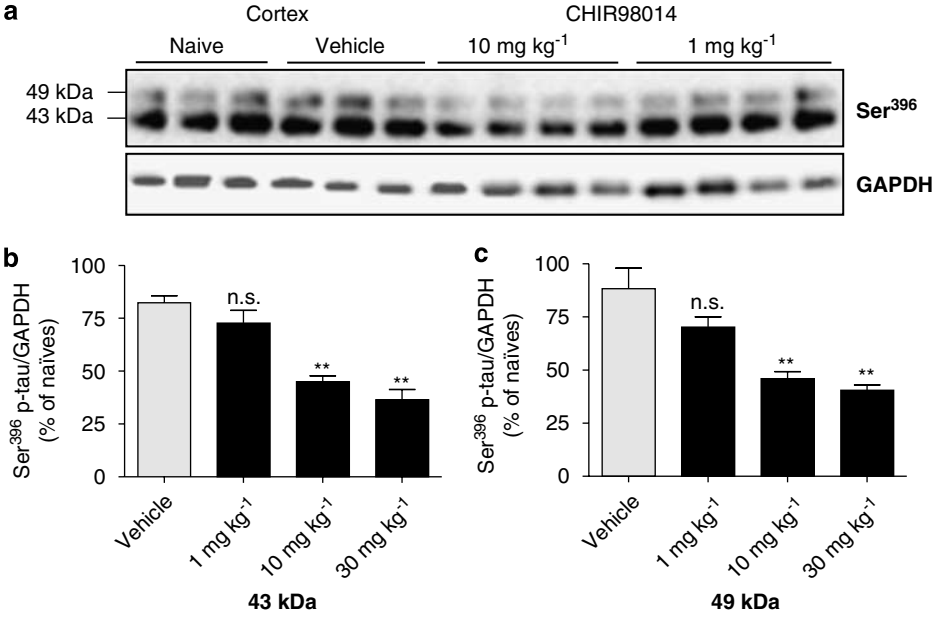

Figure 8 CHIR98014, reduced tau phosphorylation in a dose-dependent manner *in vivo*. (**a**) Three different doses of CHIR98014, 1, 10 and 30 mg kg^{-1}, were administered i.v. to P12 rats and cortical tissue was harvested after 1 h. Western blotting was performed and membranes probed with a Ser^{396} antibody to determine the dose-dependent effect of this compound on p-tau. Blots for at 1 and 10 mg kg^{-1} CHIR98014 are presented. (**b** and **c**) Quantification of Ser^{396} p-tau normalized to GAPDH is shown and represents the mean ± s.d. for both the 43 and 49 kDa bands (**$P<0.01$, NS $P>0.05$, compared to vehicle, one-way ANOVA followed by Dunnett's test; $n=4$). ANOVA, analysis of variance; GAPDH, glyceraldehyde-3-phosphate dehydrogenase; p-tau, phosphorylated tau.

Figure 9 The arylindolemaleide GSK-3 inhibitor, SB216763, reduced tau phosphorylation *in vivo*. Animals were injected i.v. with 30 mg kg^{-1} SB216763 (dissolved in DMSO) and (**a**) cortical tissue was analysed after 2 h by western blotting using a Ser^{396} p-tau-specific antibody (1:5000). (**b**) Both 43 kDa and (**c**) 49 kDa bands were quantified by densitometry. Data are expressed as Ser^{396} p-tau normalized to GAPDH and represent the mean ± s.d. (NS, $P>0.05$, *$P<0.05$, compared to vehicle-treated animals, or naive animals, as noted, one-away ANOVA, $n=4$). (**d**) Western blotting of hippocampus analysed 2 h after i.v. injection was performed and the effect of SB216763 on p-tau levels was quantified by densitometry analysis of both the 43 and 49 kDa bands and compared to p-tau levels from DMSO-treated animals (**e** and **f**). Data represent mean ± s.d. and are expressed as Ser^{396} p-tau normalized to GAPDH (**$P<0.01$, *$P>0.05$, compared to vehicle, one-away ANOVA followed by Tukey test, $n=4$). Total GSK-3β enzyme activity was measured in both cortical (**g**) and hippocampal (**h**) tissue lysates from P12 animals treated with 30 mg kg^{-1} SB216763 i.v. for 2 h. (**i** and **j**) Quantification of ^{33}P incorporated into a GS peptide was performed by densitometry analysis of autoradiographic film. Data are expressed as percentage of vehicle-treated animals and represent the mean ± s.d. (NS, $P>0.05$, *$P<0.05$, *t*-test followed by Mann–Whitney test, $n=3$). ANOVA, analysis of variance; DMSO, dimethylsulphoxide; GAPDH, glyceraldehyde-3-phosphate dehydrogenase; GS, glycogen synthase; GSK-3, glycogen synthase kinase-3; p-tau, phosphorylated tau.

immunohistochemical analysis revealed a clear pattern of enhanced tau phosphorylation throughout the postnatal rat brain. High levels of p-tau were found both in cell bodies and neurites, as reported previously (Gartner *et al.*, 1998; Takahashi *et al.*, 2000). Studies investigating the distribution of tau during development using total anti-tau antibodies (Brion *et al.*, 1994; Takahashi *et al.*, 2000) showed staining in neurons and proximal neurites in the neocortex and hippocampus of 9-day-old rats. The staining intensity in the cell soma and apical dendrites appeared to be increased

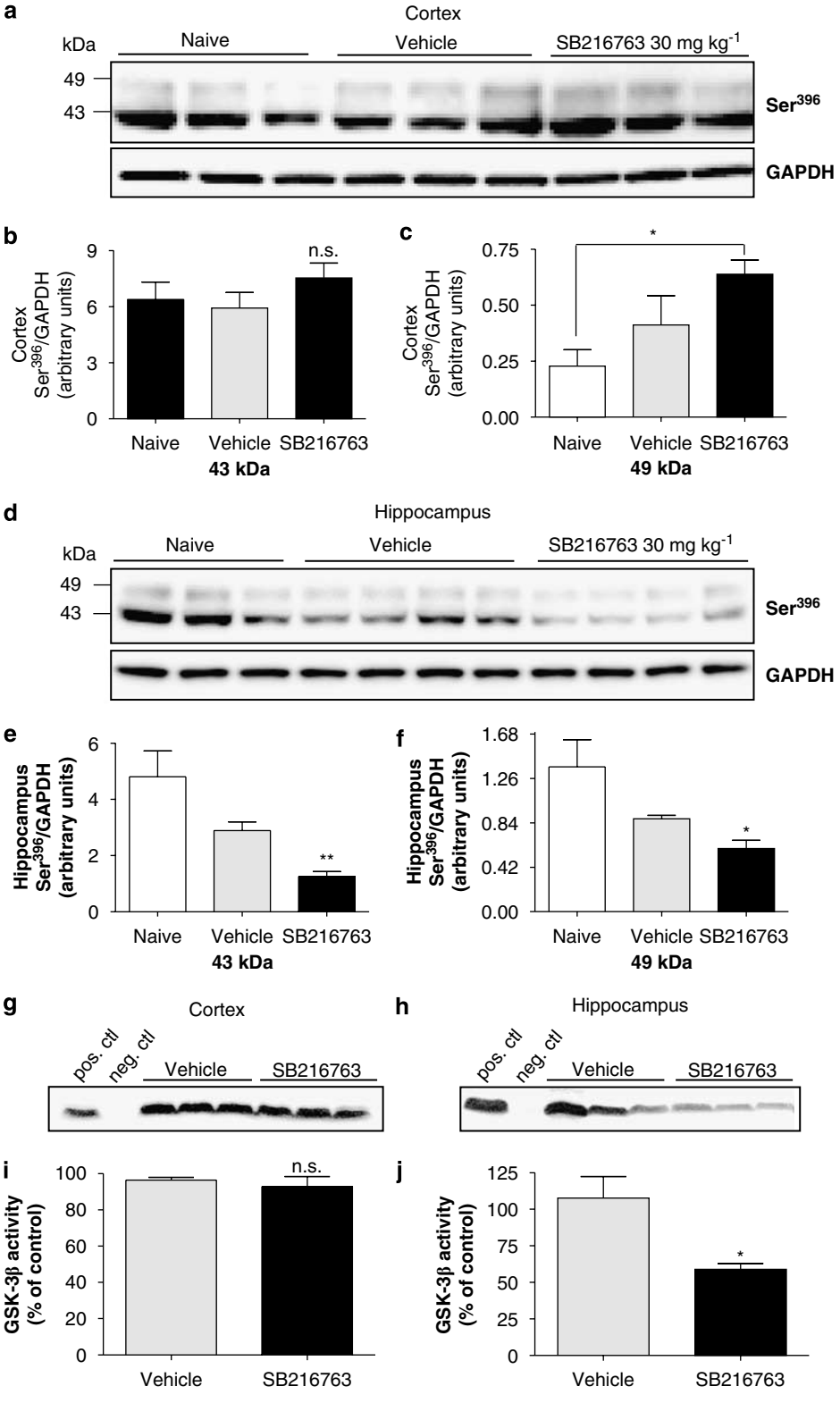

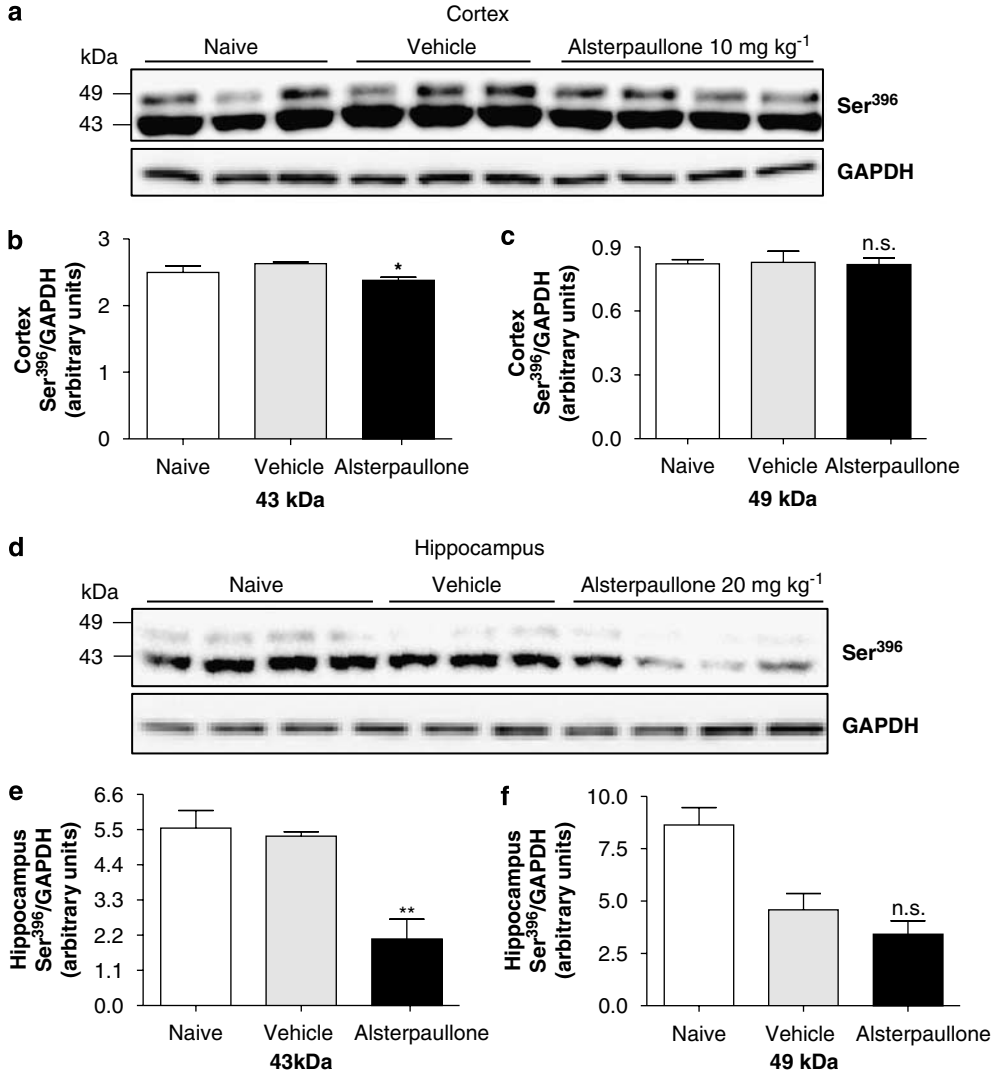

Figure 10 The benzazepinone GSK-3 inhibitor, Alsterpaullone, reduced tau phosphorylation *in vivo*. P12 rats were treated with 20 mg kg^{-1} Alsterpaullone s.c. for 1, 2 and 4 h (dissolved in 20% DMSO/25% Tween-80). (**a**) Cortical tissue analysed after 2 h by western blotting using a Ser^{396} p-tau-specific antibody (1:5000). (**b** and **c**) Quantification of 43 and 49 kDa p-tau bands was performed by densitometry analysis. Data are expressed as Ser^{396} p-tau normalized to GAPDH and represent the mean ± s.d. (*$P<0.05$, NS, $P>0.05$, compared to vehicle, one-way ANOVA, $n=4$). (**d**) Western blotting of hippocampus was analysed 2 h after drug administration as described above and (**e** and **f**) the effect of 20 mg kg^{-1} Alsterpaullone (s.c. administration) on hippocampal levels of p-tau was quantified by performing densitometry on both 43 and 49 kDa bands and compared to vehicle-treated animals. Data represent mean ± s.d. and are expressed as Ser^{396} p-tau normalized to GAPDH (**$P<0.01$, NS, $P>0.05$, compared to vehicle, one-way ANOVA followed by Tukey test, $n=4$). ANOVA, analysis of variance; DMSO, dimethylsulphoxide; GAPDH, glyceraldehyde-3-phosphate dehydrogenase; GS, glycogen synthase; GSK-3, glycogen synthase kinase-3; p-tau, phosphorylated tau.

in adult (5-week-old) rats. This differed from the staining pattern using phospho-specific antibodies, which was weaker. Similarly, in our study, the activity of GSK-3β strongly correlated with the observed increase in p-tau expression, suggesting that tau is indeed hyperphosphorylated by GSK-3β in our animal model.

To test the efficacy of pharmacological inhibition of GSK-3β on tau phosphorylation, we used several known inhibitors of GSK-3 belonging to distinct chemical classes in both a human, neuronal *in vitro* model (LUHMES cells) and in our *in vivo* rodent model. These inhibitors were chosen based on their high affinity and selectivity for GSK-3β over other, potentially related kinases (for example, CDK1, 2 and 5, PKA, PKC, MAPKK, ERK, JNK and SAPK) at concentrations relevant to those used in our recombinant assay (Coghlan *et al*., 2000; Leclerc *et al*., 2001; Martinez *et al*., 2002; Bhat *et al*., 2003). For example, Bhat *et al*. (2003) used 10 μM AR-A014418, which showed selectivity towards GSK-3β ($IC_{50}=104$ nM) over 26 other kinases. Paullones and maleimide derivatives were used at increasing concentrations, up to 100 μM and again the selectivity towards GSK-3β was found to be in the nM range. Those concentrations were well above the 2 μM concentration used in our recombinant assay. Lithium was included due to its wide use in the literature (Klein and Melton, 1996; Phiel and Klein, 2001; Jope, 2003; Beaulieu *et al*., 2004; Gould *et al*., 2006). A recombinant GSK-3β activity assay showed IC_{50} values in the nM–low μM range, correlating with published data for these compounds

(Table 2) with the exception of TDZD-8. TDZD-8, a GSK-3β inhibitor with a reported non-ATP competitive mode of action (Martinez *et al*., 2002), was completely ineffective at reducing p-tau in a human neuronal cell line or at protecting cells from the toxic effects of LY294002, a PI3 kinase inhibitor known to induce apoptosis via activation of GSK-3β, when used at 2 μM. Even though Martinez *et al*. (2002) have reported an $IC_{50} = 2\,\mu M$ in a recombinant assay, we estimated an $IC_{50} \approx 10\,\mu M$ in an immunoprecipitation-based cellular assay, which might explain its lack of efficacy in our neuronal assay.

In contrast to TDZD-8, CHIR98014, Alsterpaullone, Indirubin-3′-monoxime and SB216763 were very potent at reducing tau phosphorylation and preventing LY294002-induced cell death *in vitro*. The efficacy of SB216763 in our experiments correlates with published studies showing the ability of this compound to stimulate glycogen synthesis in human liver cells (Coghlan *et al*., 2000) and protect neuronal cells from LY294002-induced apoptosis (Cross *et al*., 2001). However, the effect of SB216763, CHIR98014, and Alsterpaullone on AD-relevant end points has not been reported in the literature. For instance, CHIR09814 has shown efficacy in rodent models of type II diabetes (Ring *et al*., 2003) but had never been tested either *in vitro* or *in vivo* for its effects on tau phosphorylation. On the other hand, Indirubin-3′-monoxime was tested in insect cells transfected with human 3R tau (Leclerc *et al*., 2001), and AR-A014418 in 3T3 fibroblasts overexpressing 4R tau (Bhat *et al*., 2003) and shown to reduce tau phosphorylation in both systems. In our human neuronal cell line, however, AR-A014418 did not reduce tau phosphorylation when used at a similar concentration of 2 μM but partially rescued cells from LY294002-induced cell death in agreement with studies by Bhat *et al*. (2003) showing protection against LY294002-induced toxicity in mouse neuroblastoma N2A cells as well as Aβ-mediated cell death in organotypic hippocampal slices at similar concentrations. Thus, it appears that inhibition of a kinase other than GSK-3β could mediate the neuroprotective effect of AR-A014418, since this compound showed an IC_{50} of 10 μM in our cell-based enzyme activity assay. This target remains elusive and does not appear to include one of the 26 kinases tested by Bhat *et al*. (2003) in a crossreactivity screen performed at 10 μM.

Next, we investigated whether pharmacological inhibition of GSK-3β *in vivo* could reduce tau phosphorylation in this model and whether this effect was directly linked to inactivation of the enzyme. LiCl and CHIR98014 dose dependently decreased p-tau levels in the hippocampus and cortex. In the cortex, the effect on 43 and 49 kDa tau isoforms was comparable, but in the hippocampus, both inhibitors led to a greater reduction in the 43 vs the 49 kDa p-tau band in the hippocampus, suggesting that in this brain region, the shorter isoform of tau is a better substrate for GSK-3β. *Ex vivo* GSK-3β activity assays performed in cortical tissue showed a 40–50% decrease in enzyme activity following administration of these compounds. Interestingly, SB216763 reduced tau phosphorylation of both 43 and 49 kDa isoforms (although an effect on the latter was more pronounced) in the hippocampus but not cortex with GSK-3β activity measurements showing a positive correlation between p-tau reduction and GSK-3β inhibition in these regions. Although we cannot offer a clear explanation as to why GSK-3β activity was reduced in one brain area and not in the other, it is possible that the inhibitory mode of action of this compound is dependent on the phosphorylation state of the enzyme, for example GSK-3β activity is normally inhibited by phosphorylation at Ser^9 by kinases such as Akt and activated by auto-phosphorylation at Tyr^{216} (Cross *et al*., 1995; Lochhead *et al*., 2006), and that the basal activity of GSK-3β and distribution of kinases modulating GSK-3β phosphorylation (for example, PKB/Akt and PKA) could differ across brain regions. Also, the tissue distribution of the compounds may account for some of the discrepancy in their effects on p-tau levels (that is, hippocampus vs cortex). In addition, the differential expression of other tau-phosphorylating kinases such as CDK5 in these areas could play a role.

Unlike several of the inhibitors tested, AR-A014418 showed no effect in reducing tau phosphorylation *in vivo* at doses where the compound reached low μM concentrations in the brain (Figure 5). Since our cell-based activity assay showed an IC_{50} 100-fold higher than that reported in the literature and confirmed in-house using a recombinant GSK-3β activity assay, we hypothesize that this inhibitor could be significantly metabolized or degraded in the media or inside the cell, as an assay in Caco-2 cells showed modest membrane permeability for this compound (data not shown). Indeed, its lack of efficacy in reducing tau phosphorylation in our neuronal *in vitro* model supports this hypothesis. Interestingly, AR-A014418 was shown to decrease aggregated p-tau in the brainstem of JNPL3 transgenic mice (Noble *et al*., 2005) and reverse defects in axonal transport in a *Drosophila* model (Mudher *et al*., 2004). Since different vehicles were used for these studies and the authors did not report CNS levels in their model systems we cannot draw any conclusions regarding the discrepancies observed between studies. However, we suggest that the effects observed by both groups could be mediated by an interaction of AR-A1014418 with other kinases besides GSK-3β, since we also found that AR-A1014418 rescued the LUHMES cells from LY294002 toxicity at a concentration where this enzyme was not inhibited. Indirubin-3′-monoxime also did not have an effect on p-tau levels in our postnatal rat model despite its efficacy *in vitro* and μM exposure levels in the brain, well above its IC_{50}, with one of the vehicles tested (Table 1).

Diverse transgenic mice models overexpressing mutant forms of tau have been developed in order to elucidate the mechanism behind tau pathology in neurodegenerative diseases such as FTDP-17 and AD (Spittaels *et al*., 1999; Ikeda *et al*., 2005; Boekhoorn *et al*., 2006). In an inducible model, suppression of mutated tau overexpression led to improvements in memory function and neuroprotection despite the ongoing presence of NFT (Ramsden *et al*., 2005; SantaCruz *et al*., 2005). Other models of tau mutations show synaptic dysfunction and gliosis during early age when tangles are still not present (Yoshiyama *et al*., 2007). These studies support the hypothesis that pre-aggregated forms of tau could be responsible for synaptic deficits and cognitive dysfunction, effects that could be mediated by axonal transport defects and are independent of NFT formation.

In this study, we present for the first time, evidence for the *in vivo* effect of six classes of small-molecule GSK-3 inhibitors on reducing tau hyperphosphorylation in a postnatal rat model and a human neuronal cell line. The effect on tau phosphorylation *in vivo* was observed in regions relevant to the pathogenesis of AD and at brain concentrations within the IC_{50} range of these compounds. The target selectivity of some of these compounds is strongly suggested by previously published reports (for references see Table 2) as well as by a small crossreactivity screen assay performed by us (data not shown). The potency of the compounds was suggested by their inhibitory effect on GSK-3β activity *ex vivo* (Figures 7g, h and 9g–j) and by their positive effect on neuroprotection and reduction of p-tau levels *in vitro* at low μM concentrations. Our results support previous suggestions that GSK-3b could be an attractive target for novel disease-modifying therapies for AD and related conditions involving p-tau.

Acknowledgements

We thank Kirsten Jørgensen, Pia Møller Carstensen and Lone Lind Hansen for their excellent technical help, Drs Christoffer Bundgaard for help with the PK analyses, Dr Claus Tornby Christoffersen for help on setting up the GSK-3β activity assay and Dr Rene Holm for advice on vehicles and routes of administration. We also thank Drs Johan Van Beek and Jan Egebjerg for insightful comments to the manuscript. This work was partially supported by the Medicon Valley Academy and the Swedish Science Research Council (Project no. 05196).

Conflict of interest

The authors state no conflict of interest.

References

Arriagada PV, Growdon JH, Hedley-Whyte ET, Hyman BT (1992). Neurofibrillary tangles but not senile plaques parallel duration and severity of Alzheimer's disease. *Neurology* **42**: 631–639.

Bancher C, Brunner C, Lassmann H, Budka H, Jellinger K, Wiche G *et al.* (1989). Accumulation of abnormally phosphorylated tau precedes the formation of neurofibrillary tangles in Alzheimer's disease13. *Brain Res* **477**: 90–99.

Baumann K, Mandelkow EM, Biernat J, Piwnica-Worms H, Mandelkow E (1993). Abnormal Alzheimer-like phosphorylation of tau-protein by cyclin-dependent kinases cdk2 and cdk5. *FEBS Lett* **336**: 417–424.

Beaulieu JM, Sotnikova TD, Yao WD, Kockeritz L, Woodgett JR, Gainetdinov RR *et al.* (2004). Lithium antagonizes dopamine-dependent behaviors mediated by an AKT/glycogen synthase kinase 3 signaling cascade. *Proc Natl Acad Sci USA* **101**: 5099–5104.

Bhat R, Xue Y, Berg S, Hellberg S, Ormo M, Nilsson Y *et al.* (2003). Structural insights and biological effects of glycogen synthase kinase 3-specific inhibitor AR-A014418. *J Biol Chem* **278**: 45937–45945.

Boekhoorn K, Terwel D, Biemans B, Borghgraef P, Wiegert O, Ramakers GJ *et al.* (2006). Improved long-term potentiation and memory in young tau-P301L transgenic mice before onset of hyperphosphorylation and tauopathy. *J Neurosci* **26**: 3514–3523.

Braak H, Braak E (1991). Neuropathological stageing of Alzheimer-related changes. *Acta Neuropathol (Berl)* **82**: 239–259.

Bramblett GT, Goedert M, Jakes R, Merrick SE, Trojanowski JQ, Lee VM (1993). Abnormal tau phosphorylation at Ser396 in Alzheimer's disease recapitulates development and contributes to reduced microtubule binding 151. *Neuron* **10**: 1089–1099.

Brandt R, Leschik J (2004). Functional interactions of tau and their relevance for Alzheimer's disease 2. *Curr Alzheimer Res* **1**: 255–269.

Brandt R (1996). The tau proteins in neuronal growth and development. *Front Biosci* **1**: d118–d130.

Brion JP, Octave JN, Couck AM (1994). Distribution of the phosphorylated microtubule-associated protein tau in developing cortical neurons. *Neuroscience* **63**: 895–909.

Coghlan MP, Culbert AA, Cross DA, Corcoran SL, Yates JW, Pearce NJ *et al.* (2000). Selective small molecule inhibitors of glycogen synthase kinase-3 modulate glycogen metabolism and gene transcription. *Chem Biol* **7**: 793–803.

Cross DA, Alessi DR, Cohen P, Andjelkovich M, Hemmings BA (1995). Inhibition of glycogen synthase kinase-3 by insulin mediated by protein kinase B. *Nature* **378**: 785–789.

Cross DA, Culbert AA, Chalmers KA, Facci L, Skaper SD, Reith AD (2001). Selective small-molecule inhibitors of glycogen synthase kinase-3 activity protect primary neurones from death. *J Neurochem* **77**: 94–102.

De Sarno SP, Li X, Jope RS (2002). Regulation of Akt and glycogen synthase kinase-3 beta phosphorylation by sodium valproate and lithium. *Neuropharmacology* **43**: 1158–1164.

Drewes G, Lichtenberg-Kraag B, Doring F, Mandelkow EM, Biernat J, Goris J *et al.* (1992). Mitogen activated protein (MAP) kinase transforms tau protein into an Alzheimer-like state. *EMBO J* **11**: 2131–2138.

Ferrer I, Gomez-Isla T, Puig B, Freixes M, Ribe E, Dalfo E *et al.* (2005). Current advances on different kinases involved in tau phosphorylation, and implications in Alzheimer's disease and tauopathies. *Curr Alzheimer Res* **2**: 3–18.

Gartner U, Janke C, Holzer M, Vanmechelen E, Arendt T (1998). Postmortem changes in the phosphorylation state of tau-protein in the rat brain. *Neurobiol Aging* **19**: 535–543.

Goedert M, Crowther RA, Spillantini MG (1998). Tau mutations cause frontotemporal dementias. *Neuron* **21**: 955–958.

Goedert M, Spillantini MG, Jakes R, Rutherford D, Crowther RA (1989). Multiple isoforms of human microtubule-associated protein tau: sequences and localization in neurofibrillary tangles of Alzheimer's disease. *Neuron* **3**: 519–526.

Gong CX, Lidsky T, Wegiel J, Zuck L, Grundke-Iqbal I, Iqbal K (2000). Phosphorylation of microtubule-associated protein tau is regulated by protein phosphatase 2A in mammalian brain. Implications for neurofibrillary degeneration in Alzheimer's disease. *J Biol Chem* **275**: 5535–5544.

Gong CX, Shaikh S, Wang JZ, Zaidi T, Grundke-Iqbal I, Iqbal K (1995). Phosphatase activity toward abnormally phosphorylated tau: decrease in Alzheimer's disease brain. *J Neurochem* **65**: 732–738.

Gould TD, Picchini AM, Einat H, Manji HK (2006). Targeting glycogen synthase kinase-3 in the CNS: implications for the development of new treatments for mood disorders. *Curr Drug Targets* **7**: 1399–1409.

Hanger DP, Betts JC, Loviny TL, Blackstock WP, Anderton BH (1998). New phosphorylation sites identified in hyperphosphorylated tau (paired helical filament-tau) from Alzheimer's disease brain using nanoelectrospray mass spectrometry. *J Neurochem* **71**: 2465–2476.

Hoeflich KP, Luo J, Rubie EA, Tsao MS, Jin O, Woodgett JR (2000). Requirement for glycogen synthase kinase-3beta in cell survival and NF-kappaB activation. *Nature* **406**: 86–90.

Hong M, Chen DC, Klein PS, Lee VM (1997). Lithium reduces tau phosphorylation by inhibition of glycogen synthase kinase-3. *J Biol Chem* **272**: 25326–25332.

Hong M, Zhukareva V, Vogelsberg-Ragaglia V, Wszolek Z, Reed L, Miller BI *et al.* (1998). Mutation-specific functional impairments in distinct tau isoforms of hereditary FTDP-17. *Science* **282**: 1914–1917.

Huang HC, Klein PS (2006). Multiple roles for glycogen synthase kinase-3 as a drug target in Alzheimer's disease. *Curr Drug Targets* **7**: 1389–1397.

Ikeda M, Shoji M, Kawarai T, Kawarabayashi T, Matsubara E, Murakami T *et al.* (2005). Accumulation of filamentous tau in the cerebral cortex of human tau R406W transgenic mice. *Am J Pathol* **166**: 521–531.

Iqbal K, Alonso AC, Chen S, Chohan MO, El-Akkad E, Gong CX *et al*. (2005). Tau pathology in Alzheimer's disease and other tauopathies. *Biochim Biophys Acta* **1739**: 198–210.

Jope RS (2003). Lithium and GSK-3: one inhibitor, two inhibitory actions, multiple outcomes. *Trends Pharmacol Sci* **24**: 441–443.

Kanai Y, Chen J, Hirokawa N (1992). Microtubule bundling by tau proteins in vivo: analysis of functional domains. *EMBO J* **11**: 3953–3961.

Klein PS, Melton DA (1996). A molecular mechanism for the effect of lithium on development. *Proc Natl Acad Sci USA* **93**: 8455–8459.

Kockeritz L, Doble B, Patel S, Woodgett JR (2006). Glycogen synthase kinase-3—an overview of an over-achieving protein kinase. *Curr Drug Targets* **7**: 1377–1388.

Leclerc S, Garnier M, Hoessel R, Marko D, Bibb JA, Snyder GL *et al*. (2001). Indirubins inhibit glycogen synthase kinase-3 beta and CDK5/p25, two protein kinases involved in abnormal tau phosphorylation in Alzheimer's disease. A property common to most cyclin-dependent kinase inhibitors? *J Biol Chem* **276**: 251–260.

Leost M, Schultz C, Link A, Wu YZ, Biernat J, Mandelkow EM *et al*. (2000). Paullones are potent inhibitors of glycogen synthase kinase-3beta and cyclin-dependent kinase 5/p25. *Eur J Biochem* **267**: 5983–5994.

Leroy K, Brion JP (1999). Developmental expression and localization of glycogen synthase kinase-3beta in rat brain. *J Chem Neuroanat* **16**: 279–293.

Liang MH, Chuang DM (2006). Differential roles of glycogen synthase kinase-3 isoforms in the regulation of transcriptional activation. *J Biol Chem* **281**: 30479–30484.

Lochhead PA, Kinstrie R, Sibbet G, Rawjee T, Morrice N, Cleghon V (2006). A chaperone-dependent GSK3beta transitional intermediate mediates activation-loop autophosphorylation. *Mol Cell* **24**: 627–633.

Lotharius J, Barg S, Wiekop P, Lundberg C, Raymon HK, Brundin P (2002). Effect of mutant alpha-synuclein on dopamine homeostasis in a new human mesencephalic cell line. *J Biol Chem* **277**: 38884–38894.

Lotharius J, Falsig J, van BJ, Payne S, Dringen R, Brundin P *et al*. (2005). Progressive degeneration of human mesencephalic neuron-derived cells triggered by dopamine-dependent oxidative stress is dependent on the mixed-lineage kinase pathway. *J Neurosci* **25**: 6329–6342.

Mandelkow EM, Biernat J, Drewes G, Gustke N, Trinczek B, Mandelkow E (1995). Tau domains, phosphorylation, and interactions with microtubules. *Neurobiol Aging* **16**: 355–362.

Martinez A, Alonso M, Castro A, Perez C, Moreno FJ (2002). First non-ATP competitive glycogen synthase kinase 3 beta (GSK-3beta) inhibitors: thiadiazolidinones (TDZD) as potential drugs for the treatment of Alzheimer's disease. *J Med Chem* **45**: 1292–1299.

Mawal-Dewan M, Henley J, Van d V, Trojanowski JQ, Lee VM (1994). The phosphorylation state of tau in the developing rat brain is regulated by phosphoprotein phosphatases. *J Biol Chem* **269**: 30981–30987.

Meijer L, Flajolet M, Greengard P (2004). Pharmacological inhibitors of glycogen synthase kinase 3. *Trends Pharmacol Sci* **25**: 471–480.

Mi K, Johnson GV (2006). The role of tau phosphorylation in the pathogenesis of Alzheimer's disease. *Curr Alzheimer Res* **3**: 449–463.

Mudher A, Shepherd D, Newman TA, Mildren P, Jukes JP, Squire A *et al*. (2004). GSK-3beta inhibition reverses axonal transport defects and behavioural phenotypes in *Drosophila*. *Mol Psychiatry* **9**: 522–530.

Munoz-Montano JR, Moreno FJ, Avila J, Az-Nido J (1997). Lithium inhibits Alzheimer's disease-like tau protein phosphorylation in neurons. *FEBS Lett* **411**: 183–188.

Noble W, Planel E, Zehr C, Olm V, Meyerson J, Suleman F *et al*. (2005). Inhibition of glycogen synthase kinase-3 by lithium correlates with reduced tauopathy and degeneration *in vivo*. *Proc Natl Acad Sci USA* **102**: 6990–6995.

Pei JJ, Braak E, Braak H, Grundke-Iqbal I, Iqbal K, Winblad B *et al*. (1999). Distribution of active glycogen synthase kinase 3beta (GSK-3beta) in brains staged for Alzheimer's disease neurofibrillary changes. *J Neuropathol Exp Neurol* **58**: 1010–1019.

Pei JJ, Tanaka T, Tung YC, Braak E, Iqbal K, Grundke-Iqbal I (1997). Distribution, levels, and activity of glycogen synthase kinase-3 in the Alzheimer's disease brain. *J Neuropathol Exp Neurol* **56**: 70–78.

Perez M, Hernandez F, Lim F, az-Nido J, Avila J (2003). Chronic lithium treatment decreases mutant tau protein aggregation in a transgenic mouse model. *J Alzheimer's Dis* **5**: 301–308.

Phiel CJ, Klein PS (2001). Molecular targets of lithium action. *Annu Rev Pharmacol Toxicol* **41**: 789–813.

Phiel CJ, Wilson CA, Lee VM, Klein PS (2003). GSK-3alpha regulates production of Alzheimer's disease amyloid-beta peptides. *Nature* **423**: 435–439.

Planel E, Yasutake K, Fujita SC, Ishiguro K (2001). Inhibition of protein phosphatase 2A overrides tau protein kinase I/glycogen synthase kinase 3 beta and cyclin-dependent kinase 5 inhibition and results in tau hyperphosphorylation in the hippocampus of starved mouse. *J Biol Chem* **276**: 34298–34306.

Plyte SE, Hughes K, Nikolakaki E, Pulverer BJ, Woodgett JR (1992). Glycogen synthase kinase-3: functions in oncogenesis and development. *Biochim Biophys Acta* **1114**: 147–162.

Rahman A, Grundke-Iqbal I, Iqbal K (2005). Phosphothreonine-212 of Alzheimer abnormally hyperphosphorylated tau is a preferred substrate of protein phosphatase-1. *Neurochem Res* **30**: 277–287.

Ramsden M, Kotilinek L, Forster C, Paulson J, McGowan E, SantaCruz K *et al*. (2005). Age-dependent neurofibrillary tangle formation, neuron loss, and memory impairment in a mouse model of human tauopathy (P301L). *J Neurosci* **25**: 10637–10647.

Ring DB, Johnson KW, Henriksen EJ, Nuss JM, Goff D, Kinnick TR *et al*. (2003). Selective glycogen synthase kinase 3 inhibitors potentiate insulin activation of glucose transport and utilization *in vitro* and *in vivo*. *Diabetes* **52**: 588–595.

SantaCruz K, Lewis J, Spires T, Paulson J, Kotilinek L, Ingelsson M *et al*. (2005). Tau suppression in a neurodegenerative mouse model improves memory function. *Science* **309**: 476–481.

Spittaels K, Van den HC, Van DJ, Bruynseels K, Vandezande K, Laenen I *et al*. (1999). Prominent axonopathy in the brain and spinal cord of transgenic mice overexpressing four-repeat human tau protein. *Am J Pathol* **155**: 2153–2165.

Stambolic V, Ruel L, Woodgett JR (1996). Lithium inhibits glycogen synthase kinase-3 activity and mimics wingless signalling in intact cells. *Curr Biol* **6**: 1664–1668.

Takahashi M, Tomizawa K, Ishiguro K, Takamatsu M, Fujita SC, Imahori K (1995). Involvement of tau protein kinase I in paired helical filament-like phosphorylation of the juvenile tau in rat brain. *J Neurochem* **64**: 1759–1768.

Takahashi M, Tomizawa K, Ishiguro K (2000). Distribution of tau protein kinase I/glycogen synthase kinase-3beta, phosphatases 2A and 2B, and phosphorylated tau in the developing rat brain. *Brain Res* **857**: 193–206.

Van WJ, Haefner B (2003). Glycogen synthase kinase-3 as drug target: from wallflower to center of attention 2. *Drug News Perspect* **16**: 557–565.

Vlahos CJ, Matter WF, Hui KY, Brown RF (1994). A specific inhibitor of phosphatidylinositol 3-kinase, 2-(4-morpholinyl)-8-phenyl-4H-1-benzopyran-4-one (LY294002). *J Biol Chem* **269**: 5241–5248.

Vogelsberg-Ragaglia V, Schuck T, Trojanowski JQ, Lee VM (2001). PP2A mRNA expression is quantitatively decreased in Alzheimer's disease hippocampus. *Exp Neurol* **168**: 402–412.

Weingarten MD, Lockwood AH, Hwo SY, Kirschner MW (1975). A protein factor essential for microtubule assembly. *Proc Natl Acad Sci USA* **72**: 1858–1862.

Woodgett JR (1991). cDNA cloning and properties of glycogen synthase kinase-3. *Methods Enzymol* **200**: 564–577.

Woodgett JR (1990). Molecular cloning and expression of glycogen synthase kinase-3/factor A. *EMBO J* **9**: 2431–2438.

Yamaguchi H, Nakazato Y, Kawarabayashi T, Ishiguro K, Ihara Y, Morimatsu M *et al*. (1991). Extracellular neurofibrillary tangles associated with degenerating neurites and neuropil threads in Alzheimer-type dementia. *Acta Neuropathol (Berl)* **81**: 603–609.

Yoshiyama Y, Higuchi M, Zhang B, Huang SM, Iwata N, Saido TC *et al*. (2007). Synapse loss and microglial activation precede tangles in a P301S tauopathy mouse model. *Neuron* **53**: 337–351.